



## Research Article

# IDENTIFICATION OF THE EFFECTS AND INTERACTIONS OF FACTORS ON THE E.D.M. PROCESS IN ORDER TO MODEL IT USING TAGUCHI METHODE

**Authors:** Taoufik Kamoun , Walid Meslameni 

**To cite to this article:** Kamoun, T. & Meslameni, W. (2022). Identification of the effects and interactions of factors on the EDM process in order to model it using Taguchi method. International Journal of Engineering and Innovative Research, 4(2), p:76-103 . DOI: 10.47933/ijeir.1058096

**DOI:** 10.47933/ijeir.1058096

To link to this article: <https://dergipark.org.tr/tr/pub/ijeir/archive>



# International Journal of Engineering and Innovative Research

<http://dergipark.gov.tr/ijeir>

## IDENTIFICATION OF THE EFFECTS AND INTERACTIONS OF FACTORS ON THE E.D.M. PROCESS IN ORDER TO MODEL IT USING TAGUCHI METHODE

Taoufik Kamoun <sup>1</sup>, Walid Meslameni <sup>1\*</sup>

<sup>1</sup> Department of Mechanical Engineering, Higher Institute of Technological Studies of Sfax, ISET de Sfax, Tunisia

<https://doi.org/10.47933/ijeir.1058096>

\* Corresponding Author E-mail: meslameni.walid@gmail.com

(Received: 06.01.2022; Accepted: 07.04.2022)

**ABSTRACT:** This article presents the identification of the influence of the effects and interactions of the machining parameters (EDM) of the machine (EROTECH basic 450) in order to model the material removal rate (MRR), the tool wear rate (TWR) and the roughness of the part (Ra). We look at all the machining parameters and collect the effects by the design of experiments method. The modeling carried out is thus carried out by the response surfaces method (RSM). We use the statistical method (ANOVA) analysis of variance to approve the robustness of the models and to verify that they are statistically significant. The Taguchi method was implemented to formulate mathematical models to predict EDM machining parameters. The prediction of responses by empirical models is compared with experimental validation tests and the results are satisfactory.

**Keywords:** Experimental design, EDM, Screening, Modelling, MRR, TWR, Surface Roughness

### 1. INTRODUCTION

One of the non-traditional machining processes is electrical discharge machining (EDM) which is a widely used process in the manufacture of parts with complex shapes and parts in the material is very hard. The material removal occurs by a series of successive electric discharges, separated from each other in time, in the main and secondary machining parameters have a major influence on the workpiece and the tool during machining [1].

Numerous studies have been carried out on the process of machining by spark erosion regardless of by experimental methods [1-2-3-4-5-6-7-8-9-10-11-12-13-14] or by numerical simulations using programs such as ABACUS [15] or MATLAB [16] for different types of material.

Different types of EDM machining have been carried out to remove material from a part, mainly EDM (Sinking EDM) [1-5-6-8-9-10-11-12-17] in which an electrode in the shape to be machined is inserted into the work piece to etch hard materials, particularly wire EDM [3-4-7-13-14-18-19-20] where a moving conductor wire cuts a part along a ruled surface, especially Strip EDM [17] which uses a strip electrode to machine parts of hard materials.

In general, existing studies aimed at optimizing material removal rate (MRR), tool wear rate (TWR) and roughness (Ra) of the part of the EDM machining process by studying the influence of a number of parameters [4], the principals parameters such as the pulse time (Ton), the rest time (Toff) and the discharge current (I) and other secondary such as the distance between electrode and work piece the (GAP), duty cycle (DC), voltage (V) and parameter (TUP)

presented in Table 1, several researchers have tried to get a basic understanding on this process by developing experimental models.

**Table 1.** Research on EDM parameters

	Parameters	Studies conducted
Principal	Pulse time (Ton)	[1]-[2]-[3]-[4]-[5]-[6]-[7]-[8]-[9]-[10]-[11]-[12]-[13]-[14]-[16]
	Rest time (Toff)	[1]-[2]-[5]-[6]-[7]-[8]-[11]-[12]-[13]-[14]
	Discharge current (I)	[1]-[3]-[4]-[5]-[6]-[7]-[8]-[9]-[10]-[11]-[12]-[14]-[16]
Secondary	Distance between electrode and work piece (GAP)	[6]
	Duty cycle (DC)	[2]-[10]-[12]-[16]
	Voltage (V)	[2]-[3]-[4]-[8]-[10]-[12]-[13]
	Parameter (TUP)	[9]

Recently, there has been a sharp increase in the application of the experimental method based mainly on practical trials. Several experimental modeling techniques with varying degrees of complexity have been widely applied, such as the methodology of design of experiments with the full factorial design method [1], Taguchi [6-8-9-10-12-13-14-18-19-20], the response surfaces method (RSM) [11] and the artificial neural network method [7-12] are studied. The majority of empirical methods based primarily on practical tests are verified primarily by numerical statistical analyzes ANOVA [1-8-9-11-12-13] or by analyzes of the signal S / N ratio [6-8-9-14-18-19-20].

Indeed, many questions arise, especially with regard to the influence of a number of factors on the EDM machining process. Thus, all the experimental work carried out does not demonstrate the choice of the machining parameters retained, on the other hand they were made with the literature only, that is to say the previous research work, they consist in studying the effect of main parameters of the EDM process thus, they neglect the analysis of the impact of the effect of the secondary parameters and the effect of the various possible interactions.

In order to have a good industrial mastery of the die-sinking EDM machining process, we studied on the one hand the effects of the machining parameters, on the other hand identifying the interactions between these parameters, and finally modeling by a method statistically using the design of experiments to empirically formulate the material removal rate (MRR), tool wear rate (TWR) and roughness (Ra) of the part.

## 2. MATERIALS AND EXPERIMENTS

The experiments of this study were carried out on a die-sinking EDM machine. Experimental work begins with the identification of materials, machining response parameters and machining process parameters. Copper was chosen for the electrode and C45 unalloyed steel as the part material.

The selected EDM driving parameters were identified from a screening study of all but the most influential EDM process machining parameters.

The machining depth has been set to 1 mm and the machining time is recorded.

The output responses were identified by the material removal rate MRR, the tool wear rate TWR, and the workpiece surface roughness Ra.

The method for estimating the technical criteria of the responses is defined as follows:

- The material removal rate MRR is the rate of material ejected at the point of impact of the landfill. It is estimated from the mass of the part measured before and after machining. It is then calculated as follows:

$$\text{MRR} = \frac{(\text{Initial weight piece} - \text{Final weight piece})}{\text{Processing time}} * 60 \quad (1)$$

- The tool wear rate TWR is the ratio between the difference in the mass of the tool electrode before and after machining and the difference in the mass of the part before and after machining. is then calculated as follows:

$$TWR = \frac{(\text{Initial weight electrode} - \text{Final weight electrode})}{(\text{Initial weight piece} - \text{Final weight piece})} * 100 \quad (2)$$

- Roughness Ra is the surface finish of the part measured after machining in  $\mu\text{m}$ .

## 2.1. Study strategy

The experiments were carried out on the basis of the design of experiments approach (DOE), a two-level fractional experiment design ( $2^{8-5} + 4 = 12$  experiments), a Taguchi L16 design according to the line graph 3 two-level, and a plan with response surface methodology (RSM) and a Taguchi L27 plan according to the three-level line graph 2 were carried out in order to discover the significant factors, the possible interactions as well as the development of the mathematical models of the different answers.

## 2. 2. Test conditions

The tests were carried out on the machine (EROTECH basic 450) the material of the electrode used in this study is an electrolytic copper (ETP) electrode of rectangular shape, with the dimensions which are equal to  $80 \times 25 \times 30$  mm. The physical characteristics of this material are presented in Table 2.

**Table 2.** The properties of the electrode

Characteristics	Copper
Density ( $\text{g/cm}^3$ )	8.89
Melting temperature ( $^{\circ}\text{C}$ )	1083
Hardness (HB)	70
Electrical resistivity ( $10^{-8} \Omega\text{m}$ )	1.72

The tests were carried out with parts made of C45 steel, a steel frequently used in the manufacture of press and forging tools with a dimension which is equal to  $78 \times 60 \times 28$  mm where two tests can be carried out on each side of the part. Table 3 and Table 4 respectively provide the mechanical properties and chemical composition of C45 steel.

**Table 3.** Mechanical properties of C45 steel

Rm ( $\text{N/mm}^2$ )	Re ( $\text{N/mm}^2$ )	A (%)	Hardness (HB)	Density ( $\text{g/cm}^3$ )
560 / 620	275 / 340	14 / 16	170	7.85

C 45 steel is an unalloyed steel with a carbon content of 0.5 to 0.52%, the chemical elements present in the steel can be classified into three categories, impurities (sulfur and phosphorus), the added element (manganese) and accompanying elements (silicon) as shown in Table 4.

**Table 4.** Chemical composition of C45 steel

C	S	Mn	P	Si
0.50 – 0.52	$\leq 0.035$	0.50 – 0.80	$\leq 0.035$	0.40 maxi

The dielectric liquid used in the tests is (ELECTRA 100). It has the appropriate properties for this type of machining. The machined depth was kept constant for all tests and the machining time was measured in real time using a digital stopwatch with an accuracy of  $\pm 1$ ms. The masses of the parts and the electrodes were measured before and after treatment with a digital scale with an accuracy of  $\pm 0.01$ g. The roughness of the parts were measured by a roughness tester of the type (SRG-2000 Phase II) with a resolution of  $\pm 0.04\mu\text{m}$ .

### 3. SCREENING OF EDM MACHINING PARAMETERS

#### 3.1. Objective of the screening study

In this work, we are interested in identifying the influences of all the effects of the machining parameters of the EROTECH basic 450 machine on the responses of the material removal rate MRR, the tool wear rate TWR and the roughness Ra .

The machining parameters for the machine are numerous, classified into two categories: principal parameters and other secondary parameters (Table 5).

#### The main parameters:

- The pulse time (Ton) is the length of time during which the voltage is applied;
- The rest time (Toff) is the period during which discharges are not authorized in order to cool the electrode, remove debris, and renew the dielectric;
- The discharge current (I) is the magnitude of the current flowing through the plasma.

#### The secondary parameters:

- The duty cycle (DC) is the ratio of the discharge time to the total cycle time:

$$DC = \frac{T_{on}}{T_{on}+T_{off}} \quad (3)$$

- The (PLS) parameter is used to select the optimal evacuation signal according to the specific treatment needs;
- The electrode to work piece distance (GAP), can be identified as the distance between the electrode surface and the maximum peak of the eroded surface layer of the work piece;
- The (PRT) parameter is used to adjust the sensitivity of the protection against pollution (pollution of the GAP);
- The (TUP) TIMER UP parameter is used to adjust the stopping time, to allow the passage of the dielectric between the part and the electrode to facilitate the evacuation of burrs and the cooling of the electrode;
- The (TDW) TIMER DOWN parameter is used to set the working time which includes the duration of the approach of the electrode to the work piece and the actual duration of the discharge sequence;
- The SERVO (SRV) parameter allows adjustment of the sensitivity of the electrode feed servo system. The servo system must keep the GAP constant during machining;
- The (TWR) Timer Enable / disable parameter, that is to say activate or deactivate the protection (ENR.PROG.AUTO), an additional protection that can have a higher (Tma +) and lower (Tma-) sensitivity level ) in order to allow a more efficient cleaning of the (GAP) and quickly find the stability of the working conditions;
- The (AUX) parameter provides an auxiliary protection that allows the adjustment of the sensitivity of the protection against short circuits in the GAP;
- The (V) Volte parameter which indicates the load voltage (no-load voltage);
- The (POLARITY) polarity parameter of the electrode / part pair. By definition, the polarity is positive when the potential of the electrode-tool is greater than that of the part and negative otherwise.

**Table 5.** The maximum and minimum values of the parameters

Parameters	Values	Min/Max
Ton	4, 5, 6, 7, 8, 9, 10, 11 and 12	Min : 4 / Max : 12
Toff	3, 4, 5, 6, 7, 8 and 9	Min : 3 / Max : 9
I	3, 4, 5, 6, 7, 8, 9, 10 and 11	Min : 3 / Max : 11
PLS	0 and 1	Min : 0 / Max : 1
GAP	8, 9, 10, 11 and 12	Min : 8 / Max : 12
TUP	300 and 400	Min : 300 / Max : 400
TDW	600, 800 and 1000	Min : 600 / Max : 1000
SRV	7	-
TWR	5	-
V	2	-
AUX	6, 7, 8, 9 and 10	Min : 6 / Max : 10
POLARITE	Electrode	Positive
	Part	Negative

The cutting parameters are selected at two levels (Maxi) and (Mini) for each parameter, as shown in Table 6.

**Table 6.** Parameter levels

Parameters	Level 1	Level 2
Ton (µs)	4	12
Toff (µs)	3	9
I (A)	3	11
GAP (µm)	8	12
PLS	0	1
TUP (ms)	300	400
TDW (ms)	600	800
AUX	6	10

We used the design of experiments method. The selected plan is a screening plan a fractional factorial plan:

$$N = 2^{k-p} \tag{4}$$

- $k$ : the number of factors studied;
- 2: the number of levels per factor;
- $p$ : the number of trials in the plan was divided by  $2^p$ .

### 3.2. Choice of the experimental design

For the choice of the plan, we selected all the factors of the EDM process, that is to say eight input factors (at two levels). A Hadamard matrix ( $H_{12}$ ) was chosen, it is an orthogonal matrix, it corresponds to a fractional factorial plane ( $N = 2^{8-5}$ ) which is equal to eight experiments, this number of experiments is insufficient to determine the coefficients, we need at least nine experiments, but the order of a Hadamard matrix is necessarily 1, 2 or a multiple of 4 then we will have ( $N = 2^{8-5} + 4 = 12$  experiments), this gives a matrix of tests (A) of an  $H_{12}$  experimental design.

$$A = \begin{bmatrix} 1 & 1 & -1 & 1 & 1 & 1 & -1 & -1 \\ -1 & 1 & 1 & -1 & 1 & 1 & 1 & -1 \\ 1 & -1 & 1 & 1 & -1 & 1 & 1 & 1 \\ -1 & 1 & -1 & 1 & 1 & -1 & 1 & 1 \\ -1 & -1 & 1 & -1 & 1 & 1 & -1 & 1 \\ -1 & -1 & -1 & 1 & -1 & 1 & 1 & -1 \\ 1 & -1 & -1 & -1 & 1 & -1 & 1 & 1 \\ 1 & 1 & -1 & -1 & -1 & 1 & -1 & 1 \\ 1 & 1 & 1 & -1 & -1 & -1 & 1 & -1 \\ -1 & 1 & 1 & 1 & -1 & -1 & -1 & 1 \\ 1 & -1 & 1 & 1 & 1 & -1 & -1 & -1 \\ -1 & -1 & -1 & -1 & -1 & -1 & -1 & -1 \end{bmatrix}$$

**Table 7.** Experimental matrix for screening the parameters

N°	Factors								Reponses		
	Ton (µs)	Toff (µs)	I (A)	GAP (µm)	PLS -	TUP (ms)	TDW (ms)	AUX -	Ra (µm)	MRR (g/min)	TWR (%)
1	12	9	3	12	1	400	600	6	1.5367	0.0017	1.1905
2	4	9	11	8	1	400	800	6	3.6700	0.0614	49.631
3	12	3	11	12	0	400	800	10	4.6367	0.2415	0.0204
4	4	9	3	12	1	300	800	10	2.0300	0.0029	15.259
5	4	3	11	8	1	400	600	10	4.4267	0.0384	0.0456
6	4	3	3	12	0	400	800	6	1.7933	0.0083	10.857
7	12	3	3	8	1	300	800	10	2.6633	0.0007	6.9892

8	12	9	3	8	0	400	600	10	2.9767	0.0007	4.4025
9	12	9	11	8	0	300	800	6	3.0933	0.7847	0.0243
10	4	9	11	12	0	300	600	10	2.9367	0.0029	141.10
11	12	3	11	12	1	300	600	6	4.1667	0.1734	0.0242
12	4	3	3	8	0	300	600	6	1.8200	0.0112	8.6053

In this experimental design, we took into account the effect of eight factors in the construction of the two-level fractional factorial design in order to be able to perform the tests and subsequently measured the three responses Ra, MRR and TWR (Table 7).

### 3.3. Results and discussion

#### 3.3.1. Effect on roughness Ra

The mean effect of a factor is defined as the change in response observed when the factor changes modality. The graph of the mean effects of the factors, in Figure 1, where the mean values of Ra calculated in Table 8 have been plotted for the two levels of the factors.

**Table 8.** The average effects on Ra.

	Ton	Toff	I	GAP	PLS	TUP	TDW	AUX
Level 1	2.779	3.251	2.136	3.108	2.876	2.785	2.977	2.680
Level 2	3.178	2.707	3.821	2.850	3.082	3.173	2.981	3.278
Delta	0.399	0.544	1.685	0.258	0.206	0.388	0.004	0.598
Rang	4	3	1	6	7	5	8	2

For each factor, a line connects the means of the test results corresponding to each of the modalities in Table 7.

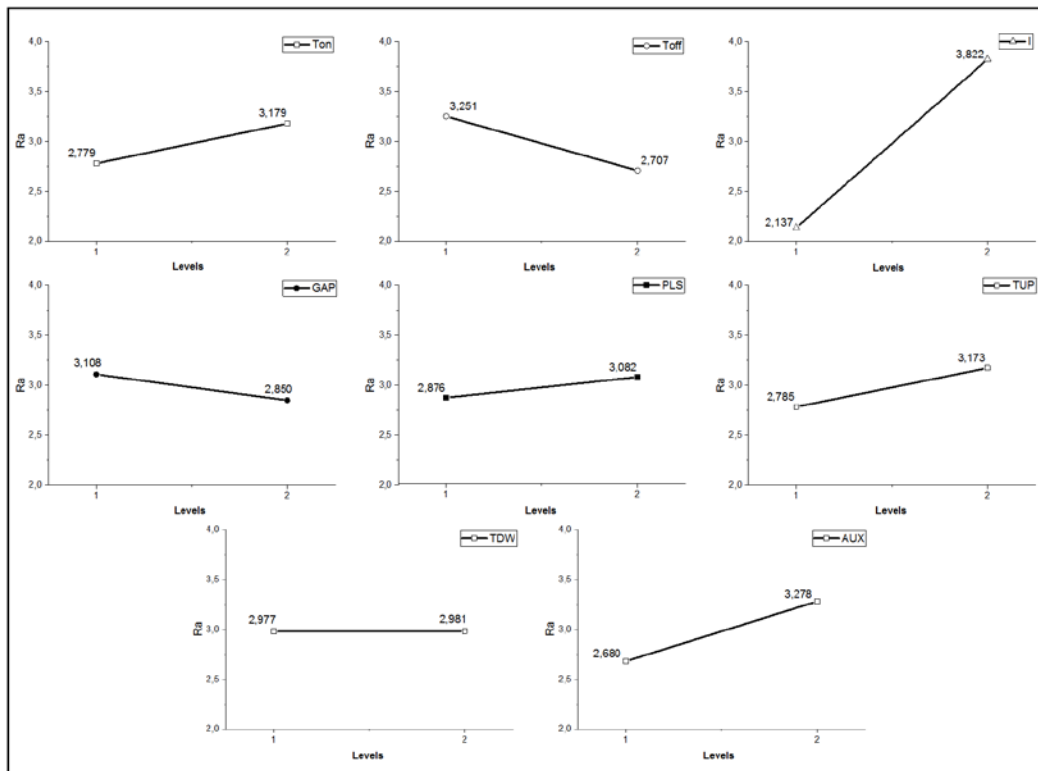


**Figure 1.** Representation of the average effects on Ra.

Table 8 of the average effects of the factors on the roughness Ra, shows that it is too influenced by the discharge current I, it reaches a maximum value for a discharge current I = 11 A, this phenomenon is easily understood since the EDM machining is based on sparking, when the value of the discharge current is increased from 3 to 11 A the size of the removed grain increases

which justifies the increasing variation of the roughness with respect to the current (Figure 1). On the other hand, the influence of the TDW parameter is less significant with a variation in roughness between the two levels, which is equal to 0.004  $\mu\text{m}$ , this variation is represented by a line almost parallel to the x-axis.

**3.3.2. Effect on the flow of material removed rate MRR**

Figure 2 shows the evolution of the average values of the MRR material removed flow rate calculated from Table 9 for the two levels 1 and 2 of the various factors.

**Table 9.** Average effects on MRR.

	Ton	Toff	I	GAP	PLS	TUP	TDW	AUX
Level 1	0.0208	0.0789	0.0042	0.1495	0.1748	0.1626	0.0380	0.1734
Level 2	0.2004	0.1423	0.2170	0.0717	0.0464	0.0586	0.1832	0.0478
Delta	0.1796	0.0634	0.2128	0.0777	0.1284	0.1039	0.1452	0.1256
Rang	2	8	1	7	4	6	3	5

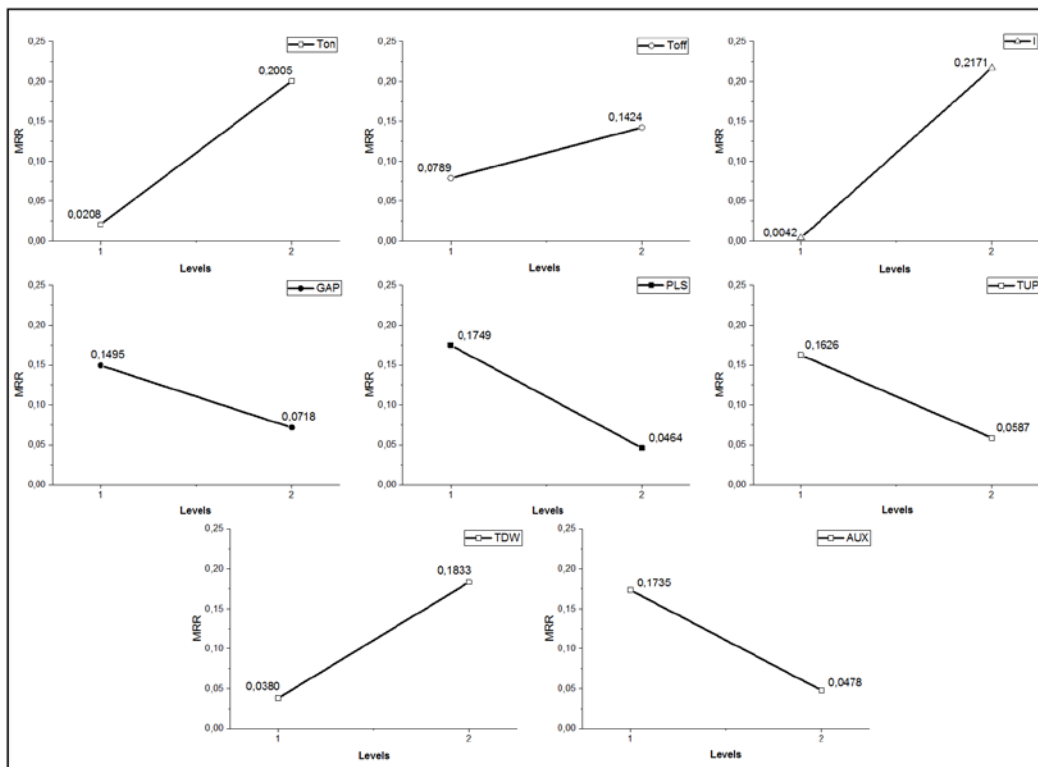


**Figure 2:** Representation of the mean effects on MRR.

The graphical representation of the average effects of the parameters on MRR in Figure 2, shows that the flow rate of material removed MRR is greatly influenced by the discharge current I, it reaches the value MRR = 0.212819 g / min for a discharge current I = 11A, while the influence of rest time Toff is less significant. It is also noted that the flow rate of material removed also admits a strong variation between the two levels of the pulse time Ton which is equal to 0.179612 g / min (Table 9).

**3.3.3. Effect on the tool wear rate TWR**

The plot of the mean factor effects, in Figure 3, represents the mean values of the TWR tool wear rate calculated from Table 10 for the two levels of the factors.



**Table 10.** The average effects on TWR.

	Ton	Toff	I	GAP	PLS	TUP	TDW	AUX
Level 1	37.583	4.423	7.883	11.616	27.501	28.667	25.894	11.722
Level 2	2.108	35.268	31.807	28.075	12.189	11.024	13.796	27.969
Delta	35.474	30.844	23.924	16.459	15.311	17.642	12.098	16.247
Rang	1	2	3	5	7	4	8	6

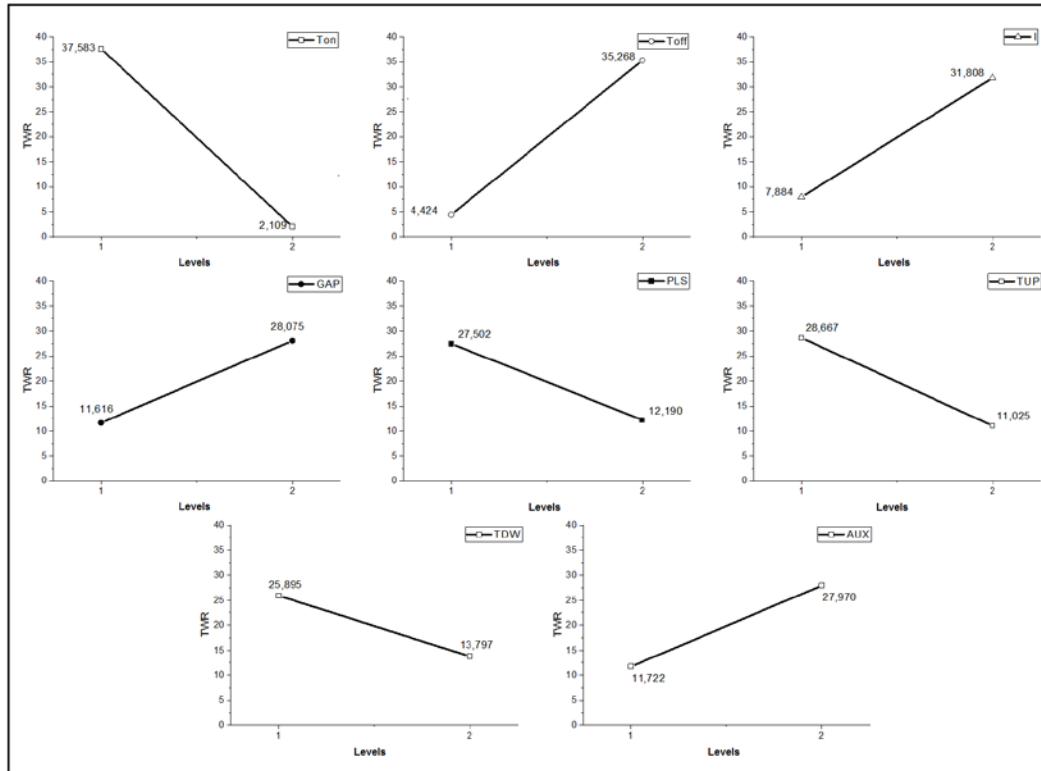


**Figure 3.** Representation of the mean effects on TWR.

The graphical representation of the average effects of the different factors on the TWR in Figure 3, shows that the TWR tool wear rate is greatly influenced by the pulse time Ton and the rest time Toff, we also notice that the discharge current I has a large effect on the variation of electrode wear rate. On the other hand, the influence of TDW time is less significant.

The diagram in Figure 4 is obtained directly from the results of the statistical analysis of the tests. The estimates of the coefficients of the first degree polynomial reflect the average effects of the factors.

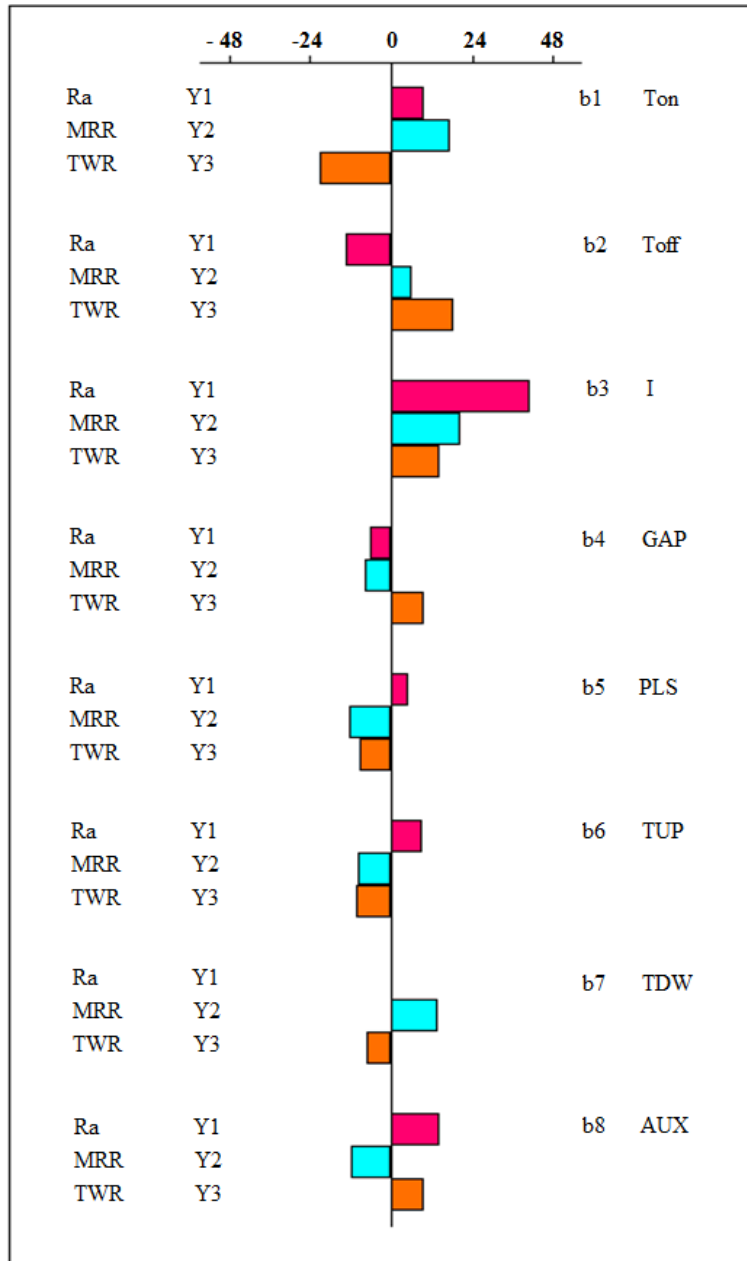


Figure 4. Effects of screening on parameters

The results of the screening tests show us that:

- The intensity of the current I is the most dominant parameter on the variation of Ra and MRR, on the other hand its effect on the TWR is less important;
- The AUX parameter has a significant effect on the response Ra, its value is very close to the value of the Toff effect;
- A weak influence for the PLS and zero for TWD on the roughness Ra, while they have an average effect on the MRR and very weak on the TWR;
- We can conclude that the parameters Ton, Toff, I and AUX turn out to have important effects.

According to the screening tests carried out, it was not possible to see the benefit of the choice of the GAP parameter among the elements of the study, but referring to the work of Kolse et al. [6] he demonstrates that the distance from the GAP varies according to the average

contamination of the GAP and also according to the parameters of the process. So that's why we added the GAP parameter to our study.

Among the 8 potentially influencing factors identified, we therefore identified 5 factors having a significant influence on the three responses.

We notice that the parameters Ton, Toff, I and AUX seem to have important effects, with regard to the others, we can say that they are weak and on any TWD.

#### 4. SCREENING OF INTERACTION FOR THE FACTORS SELECTED

##### 4.1. Objective

In a complex system, the parameters are often coupled, knowledge of the effects of each parameter is not sufficient to be able to estimate the responses. Information is therefore needed on the influence of the variation in each of the factors on the effect of the other factors, this notion called interaction.

The aim of this part is to study the interactions of order 2 between the electro erosion parameters selected in the study of the parameter screening in order to eliminate the negligible interactions. The five machining parameters are chosen at two levels as shown in Table 11.

**Table 11:** Matrix of interaction screening levels.

	I	Ton	Toff	GAP	AUX
Level 1	3	4	3	8	6
Level 2	11	12	9	12	10

##### 4.2. Choice of the experimental design

The orthogonal L16 table is chosen according to the Taguchi design with five input factors that were selected in this study. According to the line graphs in this table, it can expect up to 10 interactions. We then chose a fractional factorial design L16 which corresponds to a number of trials of 16 experiments which is represented by the trial matrix (B).

$$B = \begin{bmatrix} -1 & -1 & -1 & -1 & -1 & -1 & -1 & -1 & -1 & -1 & -1 & -1 & -1 & -1 & -1 \\ -1 & -1 & -1 & -1 & -1 & -1 & -1 & 1 & 1 & 1 & 1 & 1 & 1 & 1 & 1 \\ -1 & -1 & -1 & 1 & 1 & 1 & 1 & -1 & -1 & -1 & -1 & 1 & 1 & 1 & 1 \\ -1 & -1 & -1 & 1 & 1 & 1 & 1 & 1 & 1 & 1 & 1 & -1 & -1 & -1 & -1 \\ -1 & 1 & 1 & -1 & -1 & 1 & 1 & -1 & -1 & 1 & 1 & -1 & -1 & 1 & 1 \\ -1 & 1 & 1 & -1 & -1 & 1 & 1 & 1 & 1 & -1 & -1 & 1 & 1 & -1 & -1 \\ -1 & 1 & 1 & 1 & 1 & -1 & -1 & -1 & -1 & 1 & 1 & 1 & 1 & -1 & -1 \\ -1 & 1 & 1 & 1 & 1 & -1 & -1 & 1 & 1 & -1 & -1 & -1 & -1 & 1 & -1 \\ 1 & -1 & 1 & -1 & 1 & -1 & 1 & -1 & 1 & -1 & 1 & -1 & 1 & -1 & 1 \\ 1 & -1 & 1 & -1 & 1 & -1 & 1 & 1 & -1 & 1 & -1 & 1 & -1 & 1 & 1 \\ 1 & -1 & 1 & 1 & -1 & 1 & -1 & -1 & 1 & -1 & 1 & 1 & -1 & 1 & -1 \\ 1 & -1 & 1 & 1 & -1 & 1 & -1 & 1 & -1 & 1 & -1 & -1 & 1 & -1 & -1 \\ 1 & 1 & -1 & -1 & 1 & 1 & -1 & -1 & 1 & 1 & -1 & -1 & 1 & 1 & 1 \\ 1 & 1 & -1 & -1 & 1 & 1 & -1 & 1 & -1 & -1 & 1 & 1 & -1 & -1 & -1 \\ 1 & 1 & -1 & 1 & -1 & -1 & 1 & -1 & 1 & 1 & -1 & 1 & -1 & -1 & 1 \\ 1 & 1 & -1 & 1 & -1 & -1 & 1 & 1 & -1 & 1 & -1 & 1 & -1 & -1 & 1 \\ 1 & 1 & -1 & 1 & -1 & -1 & 1 & 1 & -1 & -1 & 1 & -1 & 1 & 1 & -1 \end{bmatrix}$$

Taguchi associated three line graphs with table L16 (Figure 5), which allow the choice of the model of coupling of interpretations between the factors to be studied.

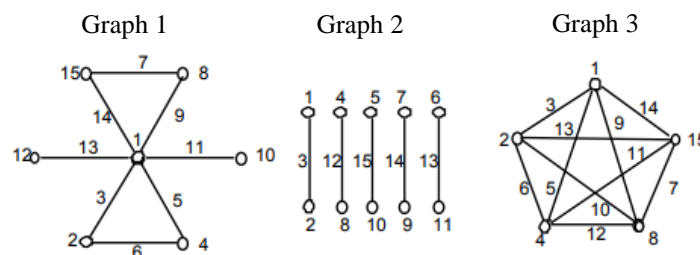


**Figure 5.** Taguchi L16 line graphs.

With 5 factors and 10 interactions, Taguchi's graph 3 meets the need for the study, to test all interactions between machine parameters. Table 12 illustrates the distribution of factors according to line graph 3 and Table 13 illustrates the experimental plan for the tests to be carried out.

**Table 12.** Matrix interaction screening experiment.

	1	2	3	4	5	6	7	8	9	10	11	12	13	14	15
N°	I	TON	I-TON	TOFF	I-TOFF	TON-TOFF	GAP-AUX	GAP	I-GAP	TON-GAP	TOFF-AUX	TOFF-GAP	TON-AUX	I-AUX	AUX
1	-1	-1	-1	-1	-1	-1	-1	-1	-1	-1	-1	-1	-1	-1	-1
2	-1	-1	-1	-1	-1	-1	-1	1	1	1	1	1	1	1	1
3	-1	-1	-1	1	1	1	1	-1	-1	-1	-1	1	1	1	1
4	-1	-1	-1	1	1	1	1	1	1	1	1	-1	-1	-1	-1
5	-1	1	1	-1	-1	1	1	-1	-1	1	1	-1	-1	1	1
6	-1	1	1	-1	-1	1	1	1	1	-1	-1	1	1	-1	-1
7	-1	1	1	1	1	-1	-1	-1	-1	1	1	1	1	-1	-1
8	-1	1	1	1	1	-1	-1	1	1	-1	-1	-1	-1	1	1
9	1	-1	1	-1	1	-1	1	-1	1	-1	1	-1	1	-1	1
10	1	-1	1	-1	1	-1	1	1	-1	1	-1	1	-1	1	-1
11	1	-1	1	1	-1	1	-1	-1	1	-1	1	1	-1	1	-1
12	1	-1	1	1	-1	1	-1	1	-1	1	-1	-1	1	-1	1
13	1	1	-1	-1	1	1	-1	-1	1	1	-1	-1	1	1	-1
14	1	1	-1	-1	1	1	-1	1	-1	-1	1	1	-1	-1	1
15	1	1	-1	1	-1	-1	1	-1	1	1	-1	1	-1	-1	1
16	1	1	-1	1	-1	-1	1	1	-1	-1	1	-1	1	1	-1

The experimental plan is therefore presented in Table 13.

**Table 13.** Experimental plan for screening interactions

N°	1	2	4	8	15	Reponses		
	I	TON	TOFF	GAP	AUX	Ra (µm)	MRR(g/min)	TWR (%)
1	3	4	3	8	6	1.7300	0.0193	9.5833
2	3	4	3	12	10	1.7800	0.0205	6.6874
3	3	4	9	8	10	2.3166	0.0021	38.8185
4	3	4	9	12	6	2.5633	0.0034	24.4196
5	3	12	3	8	10	2.8933	0.0008	10.9649
6	3	12	3	12	6	1.5000	0.0033	2.7933
7	3	12	9	8	6	1.3133	0.0039	203.653
8	3	12	9	12	10	3.0333	0.0005	5.6604
9	11	4	3	8	10	4.7200	0.0564	0.5208
10	11	4	3	12	6	4.0433	0.1533	61.1594
11	11	4	9	8	6	3.7566	0.0418	85.2833
12	11	4	9	12	10	3.2800	0.0779	59.4096
13	11	12	3	8	6	3.7466	0.6888	0.0233
14	11	12	3	12	10	3.5800	0.4103	0.0177
15	11	12	9	8	10	3.5400	1.3151	0.0287
16	11	12	9	12	6	4.3233	0.9676	0.0327

#### 4.4. Results and discussion

The aim of this analysis is to identify the interactions having a statistically significant influence on the observed responses Ra, MRR and TWR.

##### 4.4.1. Interactions of machining parameters with Roughness Ra

To facilitate the analysis of the effects of the interactions, we plotted the graphs of the interactions between the 5 parameters selected, thus, we obtained the graphs of Figure 6 which are associated with the effects of the interactions for the roughness Ra.

The examination of the graphs of the interactions of the EDM machining parameters on the roughness Ra in Figure 6 first shows the existence of the possible interactions between the

discharge current I and the other parameters AUX, GAP, Toff and Ton the most strong is to detect between the discharge current I and the auxiliary protection AUX, in the second step we also track the existence of two less significant interactions located between the distance between the electrode-part GAP and the rest time Toff and also between the distance the GAP workpiece electrode and the AUX auxiliary protection.

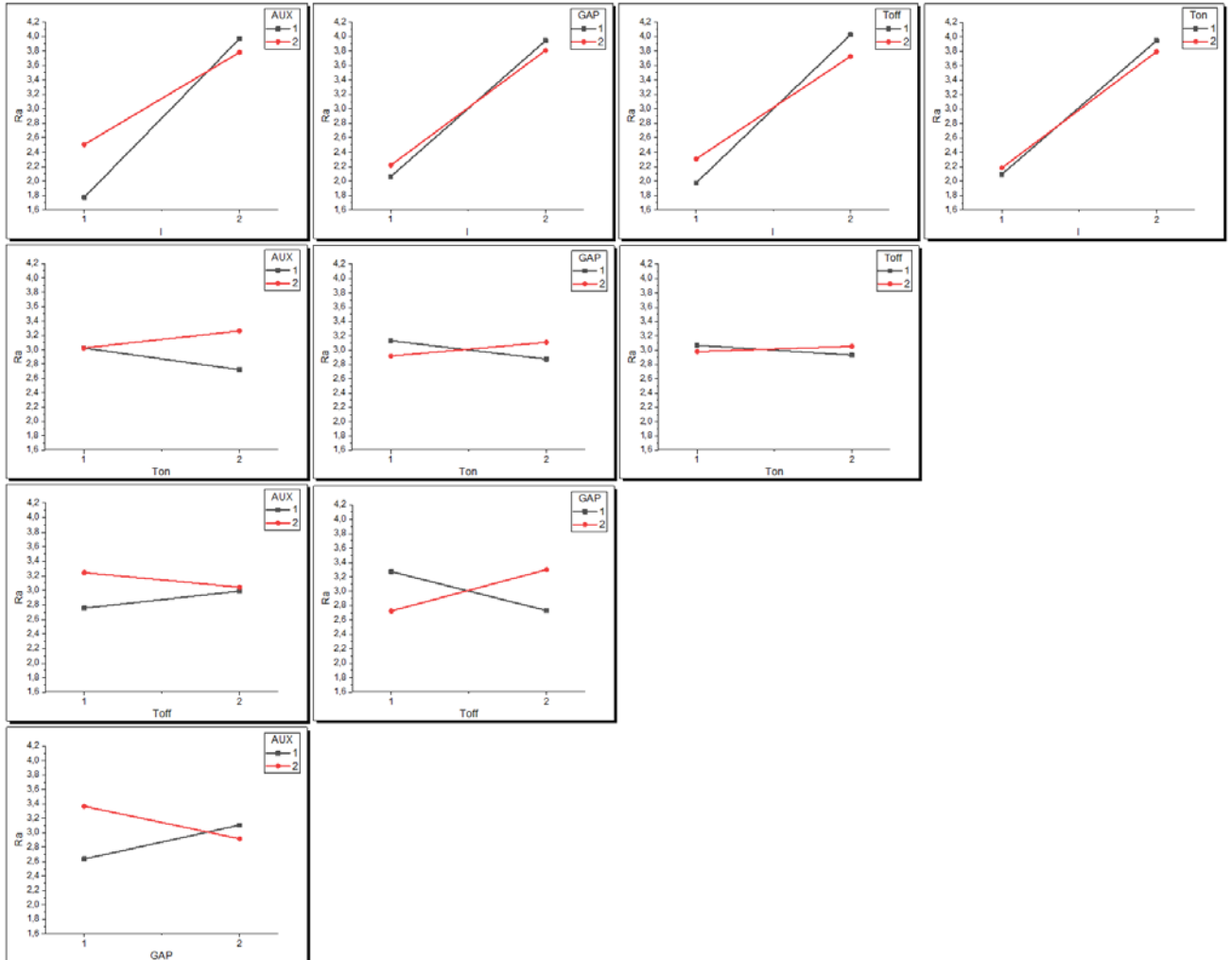


Figure 6. Graphs of interactions between EDM machining parameters for Ra

#### 4.4.2. Interactions of the machining parameters with the MRR

A strong interaction is observed in Figure 7 between the discharge current I and the pulse time Ton on the one hand, an important interaction with the Toff on the other hand, on the other hand there is no interaction between the discharge current I and AUX auxiliary protection.

Most of the interaction graphs in Figure 7 admit intersections which means the existence of interaction, but very weak compared to that of (I-Ton) and (I-Toff) except when the two lines are parallel or therefore no interaction detected.

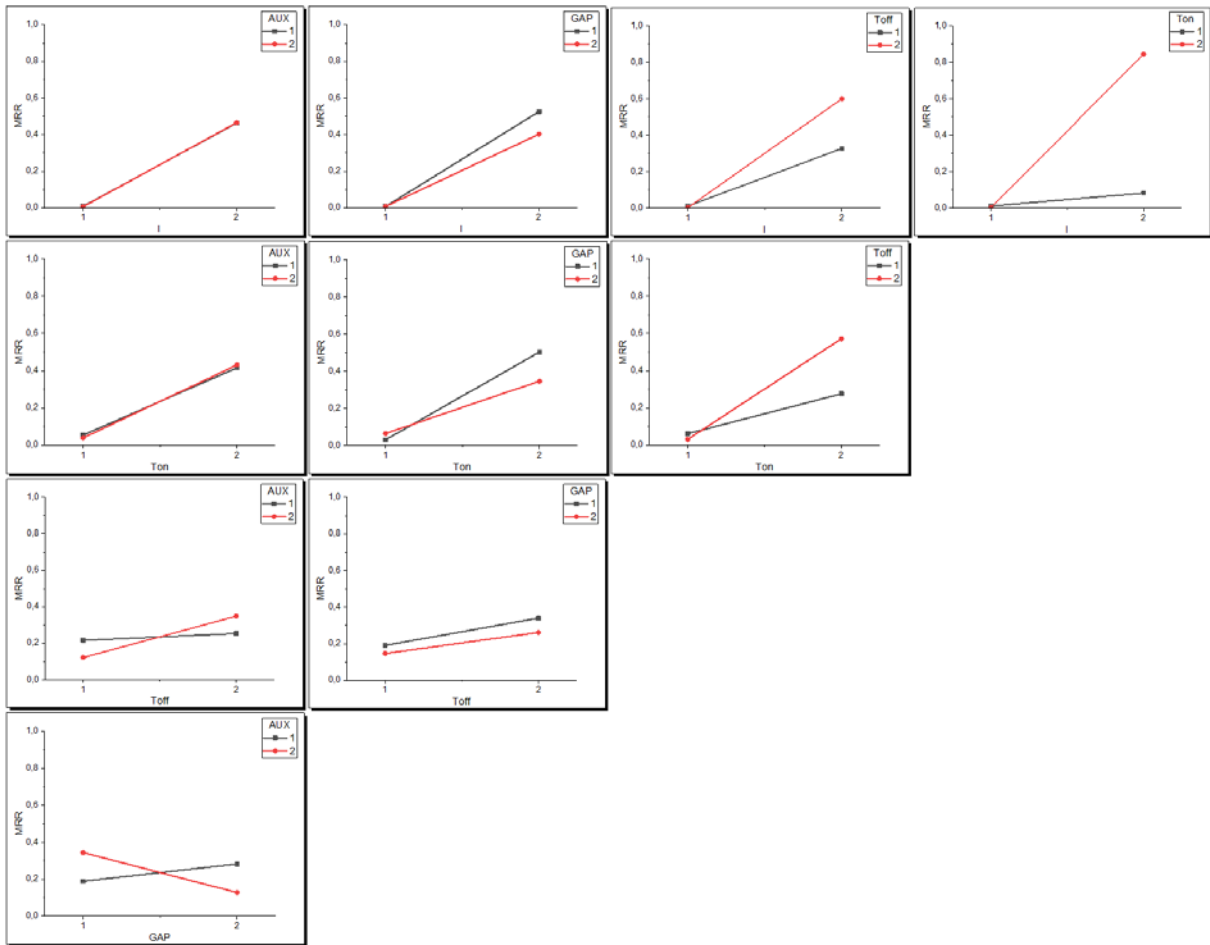


Figure 7. Graphs of interactions between EDM machining parameters for MRR.

#### 4.4.3. Interactions of machining parameters with the TWR tool wear rate

The lines of the interaction graphs in Figure 8 are not parallel or superimposed; we can conclude that there is:

- an interaction between (I-Toff), (I-GAP) and (I-Ton).
- a weak interaction between (Ton-Toff) and (I-AUX).

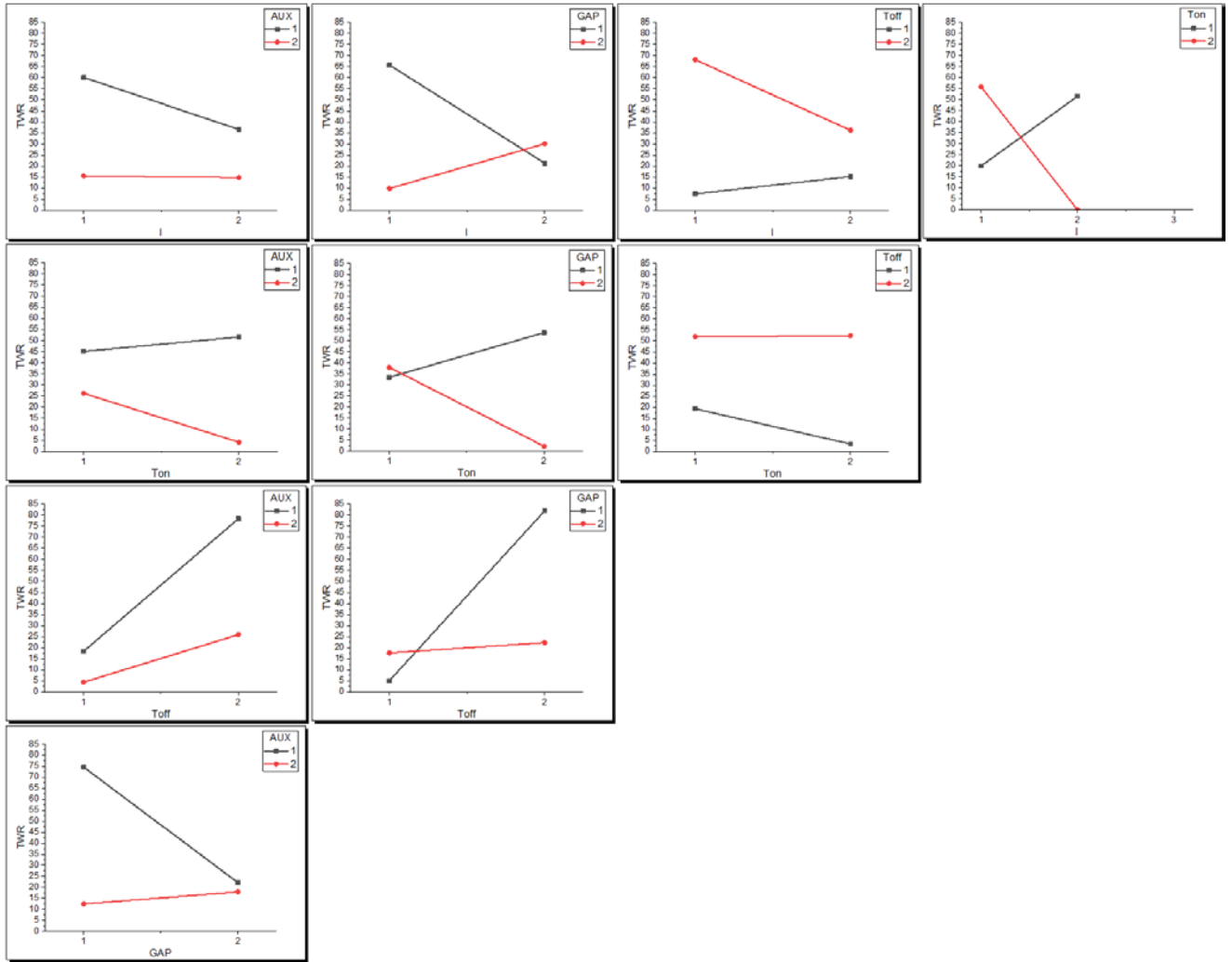


Figure 8. Graphes des interactions entre les paramètres d'usinage EDM pour TWR.

### 5. MODELING

The purpose of the Response Surface Method (RSM) is to explore the relationships between dependent and independent variables involved in the EDM machining process. After having identified the list of factors and influencing interactions and to study the response surfaces, it is necessary to increase the number of levels of the factors (to three levels) in order to better control their actions. The 5 machining parameters are chosen in three levels as shown in Table 14.

Table 14: Matrix of the levels of the response surfaces.

	I	Ton	Toff	GAP	AUX
Level 1	4	4	3	8	6
Level 2	7	8	6	10	8
Level 3	10	12	9	12	10

In the two presiding screening experiments, we noticed the existence of tests that exceed 30 hours of machining, so to limit the machining time, we limited the range of current intensity from 4 to 10 A instead of 3 to 11 A, it is also necessary to keep the same central value of the domain.

#### 5.1. Choice of the experimental design

Taguchi's experimental design L27 was chosen to study the 5 parameters I, Ton, Toff, GAP and AUX and the interactions with the discharge current (I) I-Ton, I-Toff, I-GAP and I- AUX which were selected from the preceding screening, a plan L27 which corresponds to a number of tests which is equal to 27 experiments presented by the following test matrix (C):

$$C = \begin{bmatrix} -1 & -1 & -1 & -1 & -1 & -1 & -1 & -1 & -1 & -1 & -1 & -1 & -1 & -1 \\ -1 & -1 & -1 & -1 & 0 & 0 & 0 & 0 & 0 & 0 & 0 & 0 & 0 & 0 \\ -1 & -1 & -1 & -1 & 1 & 1 & 1 & 1 & 1 & 1 & 1 & 1 & 1 & 1 \\ -1 & 0 & 0 & 0 & -1 & -1 & -1 & 0 & 0 & 0 & 1 & 1 & 1 & 1 \\ -1 & 0 & 0 & 0 & 0 & 0 & 0 & 1 & 1 & 1 & -1 & -1 & -1 & -1 \\ -1 & 0 & 0 & 0 & 1 & 1 & 1 & -1 & -1 & -1 & 0 & 0 & 0 & 0 \\ -1 & 1 & 1 & 1 & -1 & -1 & -1 & 1 & 1 & 1 & 0 & 0 & 0 & 0 \\ -1 & 1 & 1 & 1 & 0 & 0 & 0 & -1 & -1 & -1 & 1 & 1 & 1 & 1 \\ -1 & 1 & 1 & 1 & 1 & 1 & 1 & 0 & 0 & 0 & -1 & -1 & -1 & -1 \\ 0 & -1 & 0 & 1 & -1 & 0 & 1 & -1 & 0 & 1 & -1 & 0 & 1 & 0 \\ 0 & -1 & 0 & 1 & 0 & 1 & -1 & 0 & 1 & -1 & 0 & 1 & -1 & 0 \\ 0 & -1 & 0 & 1 & 1 & -1 & 0 & 1 & -1 & 0 & 1 & -1 & 0 & 0 \\ 0 & 0 & 1 & -1 & -1 & 0 & 1 & 0 & 1 & -1 & 1 & -1 & 0 & 0 \\ 0 & 0 & 1 & -1 & 0 & 1 & -1 & 1 & -1 & 0 & -1 & 0 & 1 & 0 \\ 0 & 0 & 1 & -1 & 1 & -1 & 0 & -1 & 0 & 1 & 0 & 1 & -1 & 0 \\ 0 & 1 & -1 & 0 & -1 & 0 & 1 & 1 & -1 & 0 & 0 & 1 & -1 & 0 \\ 0 & 1 & -1 & 0 & 0 & 1 & -1 & -1 & 0 & 1 & 1 & -1 & 0 & 0 \\ 0 & 1 & -1 & 0 & 1 & -1 & 0 & 0 & 1 & -1 & -1 & 0 & 1 & 0 \\ 1 & -1 & 1 & 0 & -1 & 1 & 0 & -1 & 1 & 0 & -1 & 1 & 0 & 0 \\ 1 & -1 & 1 & 0 & 0 & -1 & 1 & 0 & -1 & 1 & 0 & -1 & 1 & 0 \\ 1 & -1 & 1 & 0 & 1 & 0 & -1 & 1 & 0 & -1 & 1 & 0 & -1 & 0 \\ 1 & 0 & -1 & 1 & -1 & 1 & 0 & 0 & -1 & 1 & 1 & 0 & -1 & 0 \\ 1 & 0 & -1 & 1 & 0 & -1 & 1 & 1 & 0 & -1 & -1 & 1 & 0 & 0 \\ 1 & 0 & -1 & 1 & 1 & 0 & -1 & -1 & 1 & 0 & 0 & -1 & 1 & 0 \\ 1 & 1 & 0 & -1 & -1 & 1 & 0 & 1 & 0 & -1 & 0 & -1 & 1 & 0 \\ 1 & 1 & 0 & -1 & 0 & -1 & 1 & -1 & 1 & 0 & 1 & 0 & -1 & 0 \\ 1 & 1 & 0 & -1 & 1 & 0 & -1 & 0 & -1 & 1 & -1 & 1 & 0 & 0 \end{bmatrix}$$

Taguchi associated two line graphs for table L27 as they appear in the line graph in Figure 9.

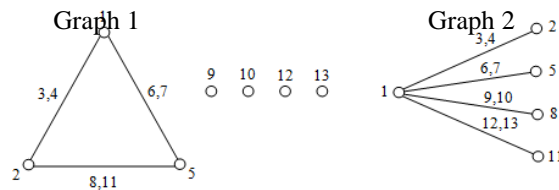


Figure 9. Taguchi L27 line graphs.

With graph 2 of the experimental design L27 only the interactions between the factors (1-2), (1-5), (1-8) and (1-11) which have a significant effect on the responses can be considered in this analysis. Table 15 illustrates the distribution of factors according to line graph 2.

Table 15. Matrix of experience of response surfaces.

	1	2	3	4	5	6	7	8	9	10	11	12	13
N° Exp	I	Ton	I-Ton	Ton-I	Toff	I-Toff	Toff-I	GAP	I-GAP	GAP-I	AUX	I-AUX	AUX-I
1	-1	-1	-1	-1	-1	-1	-1	-1	-1	-1	-1	-1	-1
2	-1	-1	-1	-1	0	0	0	0	0	0	0	0	0
3	-1	-1	-1	-1	1	1	1	1	1	1	1	1	1
4	-1	0	0	0	-1	-1	-1	0	0	0	1	1	1
5	-1	0	0	0	0	0	0	1	1	1	-1	-1	-1
6	-1	0	0	0	1	1	1	-1	-1	-1	0	0	0
7	-1	1	1	1	-1	-1	-1	1	1	1	0	0	0
8	-1	1	1	1	0	0	0	-1	-1	-1	1	1	1
9	-1	1	1	1	1	1	1	0	0	0	-1	-1	-1
10	0	-1	0	1	-1	0	1	-1	0	1	-1	0	1
11	0	-1	0	1	0	1	-1	0	1	-1	0	1	-1
12	0	-1	0	1	1	-1	0	1	-1	0	1	-1	0
13	0	0	1	-1	-1	0	1	0	1	-1	1	-1	0



14	0	0	1	-1	0	1	-1	1	-1	0	-1	0	1
15	0	0	1	-1	1	-1	0	-1	0	1	0	1	-1
16	0	1	-1	0	-1	0	1	1	-1	0	0	1	-1
17	0	1	-1	0	0	1	-1	-1	0	1	1	-1	0
18	0	1	-1	0	1	-1	0	0	1	-1	-1	0	1
19	1	-1	1	0	-1	1	0	-1	1	0	-1	1	0
20	1	-1	1	0	0	-1	1	0	-1	1	0	-1	1
21	1	-1	1	0	1	0	-1	1	0	-1	1	0	-1
22	1	0	-1	1	-1	1	0	0	-1	1	1	0	-1
23	1	0	-1	1	0	-1	1	1	0	-1	-1	1	0
24	1	0	-1	1	1	0	-1	-1	1	0	0	-1	1
25	1	1	0	-1	-1	1	0	1	0	-1	0	-1	1
26	1	1	0	-1	0	-1	1	-1	1	0	1	0	-1
27	1	1	0	-1	1	0	-1	0	-1	1	-1	1	0

### 5.2. Results and discussion

The experimental design is defined by Table 16, the results are obtained through tests planned according to the Taguchi L27 plan at three levels and two repetitions.

**Table 16.** Experimental design of response surfaces.

N°	Factors					Response					
	1	2	5	8	11	Ra (µm)		MRR (g/min)		TWR (%)	
	I	Ton	Toff	GAP	AUX	Reading 1 and 2	Mean	Reading 1 and 2	Mean	Reading 1 and 2	Mean
1	4	4	3	8	6	2.04333 2.06333	2.05333	0.04048 0.03960	0.04004	23.6434 24.5005	24.0719
2	4	4	6	10	8	2.10666 2.60333	2.35499	0.02258 0.02233	0.02246	20.3603 21.6666	21.0135
3	4	4	9	12	10	2.61333 2.38000	2.49666	0.00346 0.00331	0.00339	51.1210 50.8920	51.0065
4	4	8	3	10	10	3.26333 3.00666	3.13500	0.01592 0.01651	0.01621	5.98146 4.63576	5.30861
5	4	8	6	12	6	4.20000 3.83333	4.01666	0.03524 0.03523	0.03523	0.33333 0.46598	0.39965
6	4	8	9	8	8	4.06333 4.17333	4.11833	0.02414 0.02490	0.02452	0.85470 1.09823	0.97646
7	4	12	3	12	8	3.81666 3.83333	3.82500	0.00537 0.00429	0.00483	0.17323 0.09165	0.13244
8	4	12	6	8	10	3.89000 3.55333	3.72166	0.00131 0.00111	0.00121	12.4413 11.5755	12.0084
9	4	12	9	10	6	1.02000 0.99333	1.00666	0.00561 0.00567	0.00564	0.06389 0.06265	0.06327
10	7	4	3	8	6	3.56333 2.78333	3.17333	0.01074 0.01083	0.01078	1.06209 0.03505	0.54857
11	7	4	6	10	8	2.79333 3.03666	2.91500	0.09918 0.09542	0.09730	40.4512 39.6341	40.0427
12	7	4	9	12	10	3.10666 2.84000	2.97333	0.01696 0.01733	0.01714	67.7729 67.9462	67.8595
13	7	8	3	10	10	2.64000 3.10333	2.87166	0.10569 0.09402	0.09986	0.02844 0.03395	0.03120
14	7	8	6	12	6	4.38333 4.17333	4.27833	0.26148 0.25075	0.25612	2.51060 4.24628	3.37844
15	7	8	9	8	8	4.11666 3.99666	4.05666	0.19227 0.19040	0.19134	6.21890 6.89163	6.55527
16	7	12	3	12	8	3.68333 3.90333	3.79333	0.02363 0.02072	0.02218	0.09407 0.05903	0.07655
17	7	12	6	8	10	3.00666 4.01000	3.50833	0.25289 0.20151	0.22720	0.11444 0.02778	0.07111
18	7	12	9	10	6	3.75666 3.83000	3.79333	0.22093 0.22210	0.22151	0.03017 0.02843	0.02930
19	10	4	3	8	6	3.57333 3.32000	3.44666	0.03546 0.03682	0.03614	1.33333 0.51282	0.92307
20	10	4	6	10	8	3.66666 2.99000	3.32833	0.25370 0.23114	0.24242	49.3384 49.0419	49.1902
21	10	4	9	12	10	3.47000 3.50666	3.48833	0.04590 0.04608	0.04599	72.21750 72.47329	72.3454
22	10	8	3	10	10	3.20000 3.91333	3.55666	0.27361 0.30502	0.28932	0.019944 0.023375	0.02166
23	10	8	6	12	6	4.38333 4.28333	4.33333	0.83666 0.79569	0.81617	9.255286 9.334182	9.29473
24	10	8	9	8	8	3.42333 3.30666	3.36500	0.63275 0.60015	0.61645	20.37444 21.56306	20.9687

25	10	12	3	12	8	4.16000	4.06000	0.25503	0.24658	0.037174	0.02800
						3.96000		0.23812		0.018835	
26	10	12	6	8	10	4.23000	3.88000	1.10986	1.09733	0.021427	0.02124
						3.53000		1.08480		0.021070	
27	10	12	9	10	6	5.18666	4.89500	0.86429	0.83830	0.020550	0.02110
						4.60333		0.81231		0.021654	

The influences of the machining parameters on the material removal rate MRR, the tool wear rate TWR and the roughness Ra were studied then the robustness of the models was verified by the statistical method: analysis of variance ANOVA [22].

**5.2.1. Modeling of Ra as a function of parameters and interactions**

A polynomial roughness model has been determined, which takes into account the first and second order factors along with the interactions.

$$Ra = b_0 + b_1 \times I + b_2 \times Ton + b_3 \times I \times Ton + b_4 \times Toff + b_5 \times I \times Toff + b_6 \times GAP + b_7 \times I \times GAP + b_8 \times AUX + b_9 \times I \times AUX + b_{11} \times I^2 + b_{22} \times Ton^2 + b_{44} \times Toff^2 + b_{66} \times GAP^2 + b_{88} \times AUX^2 \quad (5)$$

The statistical analysis led us to the variance examination table in Table 17, which indicates that the model used is fitted, since the sum of squares of residuals is not small compared to the sum of the regression squares.

**Table 17.** ANOVA analysis of variance of Ra.

Source of variation	Sum of squares (SS)	Degrees of freedom (DOF)	Medium square (MS)	Rapport (F)	Signif
<b>Regression (R)</b>	25.0415	18	1.3912	<b>4.5040</b>	< 0.01 ***
<b>Residues (E)</b>	10.8107	35	0.3089		
<b>Total (T)</b>	35.8522	53			

With:

$$SS_T = SS_R + SS_E \quad (6)$$

$$MS_R = SS_R / DOF_R \quad (7)$$

$$MS_E = SS_E / DOF_E \quad (8)$$

By calculation:

$$F \text{ Ratio} = MS_R / MS_E \quad (9)$$

From the Fisher table we deduce:

$$F_{0.05} (DOF_R; DOF_E) = 1.91 < 4.5040$$

$$F_{0.01} (DOF_R; DOF_E) = 2.5 < 4.5040$$

$$F_{0.001} (DOF_R; DOF_E) = 3.38 < 4.5040 (***)$$

The Fisher test therefore makes it possible to demonstrate the existence of a statistically significant difference at the 99.9% confidence level indicated in Table 17 by the appearance of three stars in front of the significance of the regression.

To note :

- (\*) Significant value at a confidence level of 95%
- (\*\*) Significant value at a confidence level of 99%
- (\*\*\*) Significant value at a confidence level of 99.9%

In other words, the more significant the result of the hypothesis test, the more it is associated with a significant number of stars.

A more detailed analysis of the estimates and statistics of the coefficients by the multiple linear correlation coefficient R2 which is evaluated by:

$$R_2 = SS_R / SS_T = 1 - (SS_E / SS_T) \quad (10)$$

With a value between (0 ≤ R2 ≤ 1) and an excellence value R2 = 0.7.

The correlation coefficient R2 has a value, which is equal to 0.698 ≈ 0.7 (Table 18) which means that the model is fitted.

**Table 18.** Statistics of the coefficients of Ra.

Standard deviation of the response	0.5558
R2	0.698
R2A	0.543
R2 pred	0.289
PRESS	25.492
Number of degrees of freedom	35

We estimated the various parameters of the model in Table 19, for each coefficient ( $b_i$ ) or ( $b_{ij}$ ), we tested the hypothesis of their nullities.

The nullity hypothesis to test the significance of each coefficient is:

$$b_i = 0 \quad (11)$$

If the assumption of Eq. (11) is not true, it indicates that ( $X_i$ ) can be eliminated from the model. The statistical test of this hypothesis is the Student's test which leads us to calculate the value ( $t_i$ ):

$$t_i = \frac{b_i}{\text{Standard Deviation of } b_i} \quad (12)$$

Interestingly, only the interaction effect between factors (I) and (AUX) seems to be significant.

**Table 19.** Estimation of the model parameters.

Name	$b_i$	Standard Devi.	$t_i$	Signif. %
b0	3.7606	0.2508	14.99	< 0.01 ***
b1	0.4236	0.0926	4.57	< 0.01 ***
b2	0.3474	0.0926	3.75	0.0638 ***
b3	-0.1154	0.0926	-1.25	22.1
b4	0.0155	0.0926	0.17	86.8
b5	-0.1368	0.0926	-1.48	14.9
b6	0.1079	0.0926	1.16	25.2
b7	-0.1171	0.0926	-1.26	21.4
b8	-0.0758	0.0926	-0.82	41.9
b9	0.3117	0.0926	3.36	0.187 **
b11	-0.0914	0.1604	-0.57	57.3
b22	-0.4861	0.1604	-3.03	0.458 **
b44	-0.2536	0.1604	-1.58	12.3
b66	0.4931	0.1604	3.07	0.409 **
b88	-0.1669	0.1604	-1.04	30.5

According to the results obtained from Table 19, we can write the response  $R_a$  in the following form:

$$R_a = 3.7606 + 0.4236 \times I + 0.3117 \times I \times AUX - 0.4861 \times Ton^2 + 0.4931 \times GAP^2 \quad (13)$$

This model has been intentionally simplified by eliminating interaction effects and order 2 parameters deemed insignificant in the previous analysis. This makes it easier to manipulate this reduced expression while maintaining a quality of fit.

Figure 10 makes it possible to judge more precisely the quality of the adjustment made experiment by experiment. The comparison between the  $Y_{exp.}$  (measured responses) and  $Y_{calc.}$  (model predicted responses) curves of  $R_a$  confirms that the model is fitted. We can notice that the maximum difference between the calculated and experimental values of roughness almost equal  $1 \mu m$ .

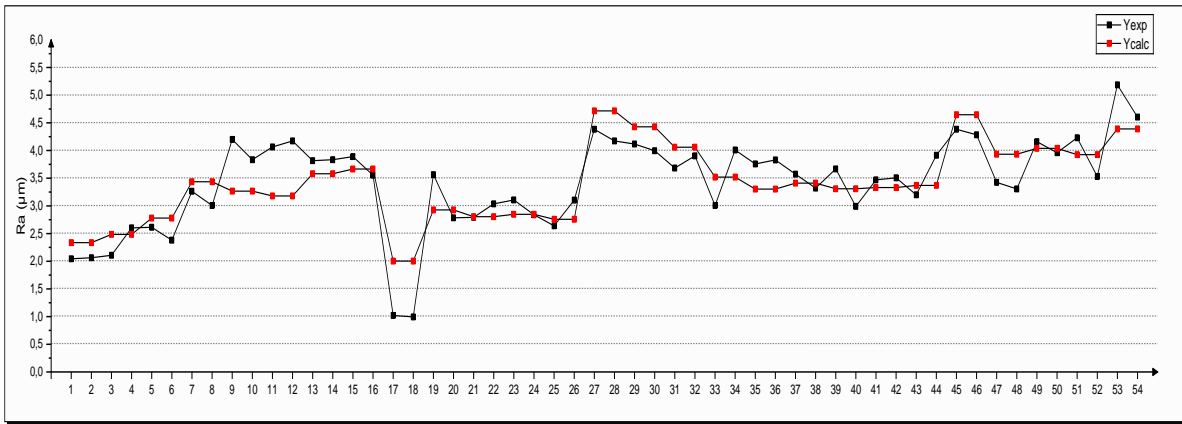
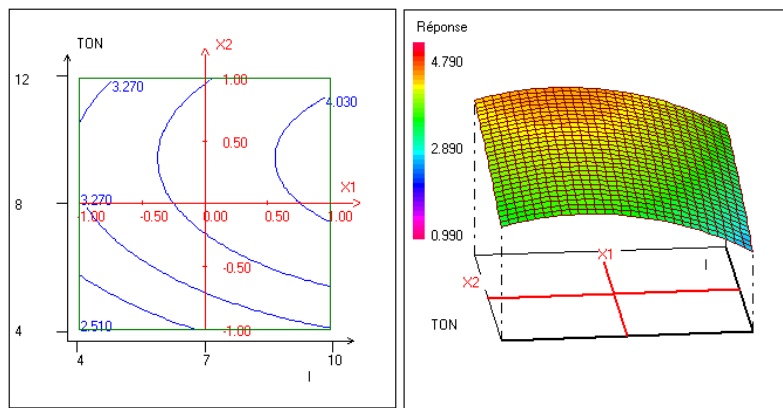


**Figure 10.** Comparison between the measured  $Y_{exp.}$  and the predicted  $Y_{calc.}$  by the model of Ra.

Response surfaces can show variations in responses based on only 2 factors at a time, with the other factors set to a fixed value. Figures 11, 12 and 13 show the response surfaces associated with the roughness model. We have chosen to present the variation of (I / Ton), (Ton / Toff) and (Toff / AUX), the other factors being fixed at the center of the experimental domain.

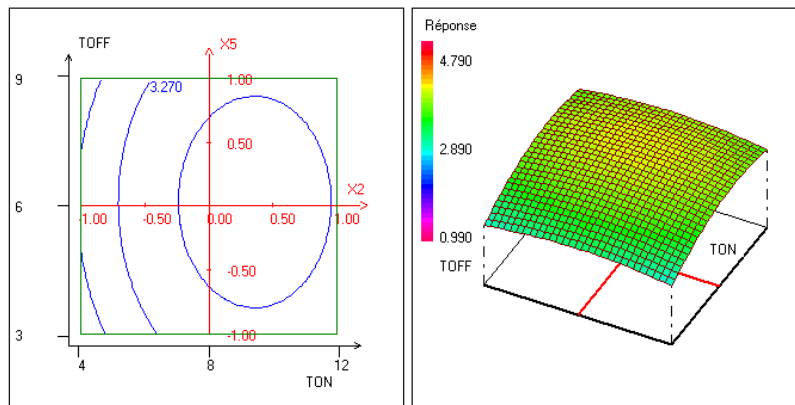
Figure 11 shows the simultaneous reproduction of the variation in discharge current and pulse time in two and three dimensions, it is observed that the optimum (minimum) of roughness is obtained when the values of I and Ton are equal to I = 4 A and Ton = 4 µs the value of the roughness Ra increases proportionally with the discharge current I.

Figure 12 shows the simultaneous two- and three-dimensional image of the pulse time variation Ton and the rest time Toff, where it can be seen that there is a stationary point almost at the center of the response surface with a maximum of roughness for the values of Ton = 8 µs and Toff = 6 µs.



**Figure 11.** 2D and 3D response surface of Ra in the I, Ton plane.

Variation of the response Ra in the I, Ton plane for the fixed factors: Toff = 6µs, GAP = 10µm, AUX = 8



**Figure 12.** 2D and 3D response surface of Ra in the Ton, Toff plane  
Variation of the response Ra in the Ton, Toff plane for the fixed factors: I = 7A, GAP = 10µm, AUX = 8

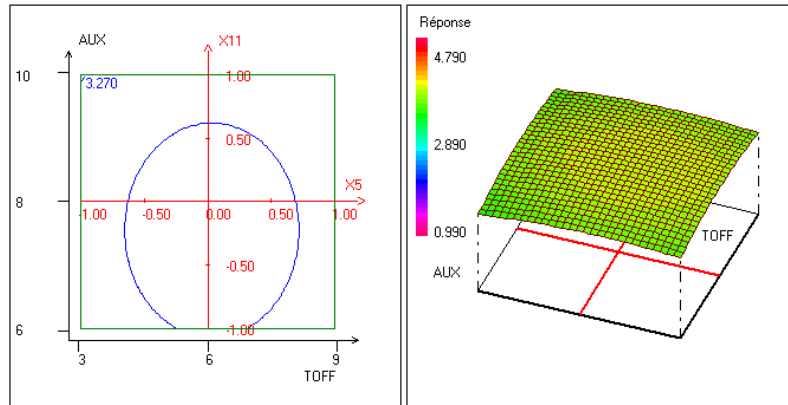


**Figure 13.** 2D and 3D response surface of Ra in the Toff plane, AUX  
Variation of the response Ra in the Toff plane, AUX. For the fixed factors: I = 7A, Ton = 8µs, GAP = 10µm.

From the simultaneous representation of Figure 13 in two and three dimensions of the variation of the rest time Toff and the auxiliary protection AUX, it can be seen that there is a stationary point almost at the center of the response surface with maximum roughness for Toff = 6 µs and AUX = 8.

**5.2.2. Modeling of MRR as a function of parameters and interactions**

We have defined a polynomial model of the material removed rate that takes into account the second order parameters and the interactions selected.

$$MRR = b_0 + b_1 \times I + b_2 \times Ton + b_3 \times I \times Ton + b_4 \times Toff + b_5 \times I \times Toff + b_6 \times GAP + b_7 \times I \times GAP + b_8 \times AUX + b_9 \times I \times AUX + b_{11} \times I^2 + b_{22} \times Ton^2 + b_{44} \times Toff^2 + b_{66} \times GAP^2 + b_{88} \times AUX^2 \quad (14)$$

The statistical analysis leads us to the analysis of variance table in Table 20. It mainly indicates that the model used is fitted, since the sum of the squares of residuals is not small compared to the sum of the regression squares.

**Table 20.** Analysis of variance of MRR.

Source of variation	Sum of squares (SS)	Degrees of freedom (DOF)	Medium square (MS)	Rapport (F)	Signif
<b>Regression (R)</b>	3.8218	18	0.2123	<b>10.6706</b>	< 0.01 ***
<b>Residues (E)</b>	0.6964	35	0.0199		
<b>Total (T)</b>	4.5182	53			

From the Fisher table, we deduce:

$$F_{0.05} (DOF_R; DOF_E) = 1.91 < 10.6706$$

$$F_{0.01} (DOF_R; DOF_E) = 2.5 < 10.6706$$

$$F_{0.001} (DOF_R; DOF_E) = 3.38 < 10.6706 (***)$$

The Fisher test, therefore, makes it possible to highlight the existence of a statistically significant difference at the 99.9% confidence level in Table 19 by the appearance of three stars in front of the significance of the regression. In other words, the more significant the result of the hypothesis test, the more it is associated with a significant number of stars.

Further analysis of the estimates and statistics of the coefficients in Table 21 gives us the result of the multiple linear correlation coefficient R2 which is equal to 0.846 a value greater than the excellence value of R2 which is acceptable which means that the model is well adjusted.

**Table 21.** Statistics of MRR coefficients.

Standard deviation of the response	0.1410593
R2	0.846
R2A	0.767
R2 pred	0.637
PRESS	1.642
Number of degrees of freedom	35

Regarding the estimation of the various parameters of the model (Table 22), for each coefficient of (bi) or (bij), we tested the hypothesis of their nullities.

Interestingly, only the interaction effect between the factors (I-Ton) and (I-TOff) seems to be significant.

**Table 22.** Estimation of the model parameters.

Name	bi	Standard Devi.	ti	Signif. %
b0	0.2464091	0.0636650	3.87	0.0453 ***
b1	0.2263984	0.0235099	9.63	< 0.01 ***
b2	0.1193956	0.0235099	5.08	< 0.01 ***
b3	-0.0763985	0.0235099	-3.25	0.255 **
b4	0.0665743	0.0235099	2.83	0.762 **
b5	-0.0811561	0.0235099	-3.45	0.147 **
b6	-0.0442989	0.0235099	-1.88	6.8
b7	0.0267111	0.0235099	1.14	26.4
b8	-0.0256834	0.0235099	-1.09	28.2
b9	0.0273157	0.0235099	1.16	25.3
b11	0.1164086	0.0407203	2.86	0.712 **
b22	-0.0838891	0.0407203	-2.06	4.69 *
b44	-0.1589255	0.0407203	-3.90	0.0413 ***
b66	0.0014777	0.0407203	0.04	97.1
b88	0.0623021	0.0407203	1.53	13.5

According to the results obtained from Table 22, the response MRR is then written in the following form:

$$\text{MRR} = 0.2464091 + 0.2263984 \times I + 0.1193956 \times \text{Ton} - 0.0763985 \times I \times \text{Ton} + 0.0665743 \times \text{Toff} - 0.0811561 \times I \times \text{Toff} + 0.1164086 \times I^2 - 0.0838891 \times \text{Ton}^2 - 0.1589255 \times \text{Toff}^2 \quad (15)$$

This model was simplified by eliminating the interaction effects and the second-order parameters deemed insignificant in the previous analysis. This makes it easier to manipulate this reduced expression while maintaining a quality of fit.

Figure 14 allows a more precise judgment of the quality of the adjustment made experiment by experiment. The comparison between the  $Y_{\text{exp}}$  (measured responses) and  $Y_{\text{calc}}$  (model predicted responses) curves of MRR confirms that the moderately fitted model.

It can be noted that the maximum difference between the calculated and experimental values of the material flow rate removed can be 0.2 g / min.

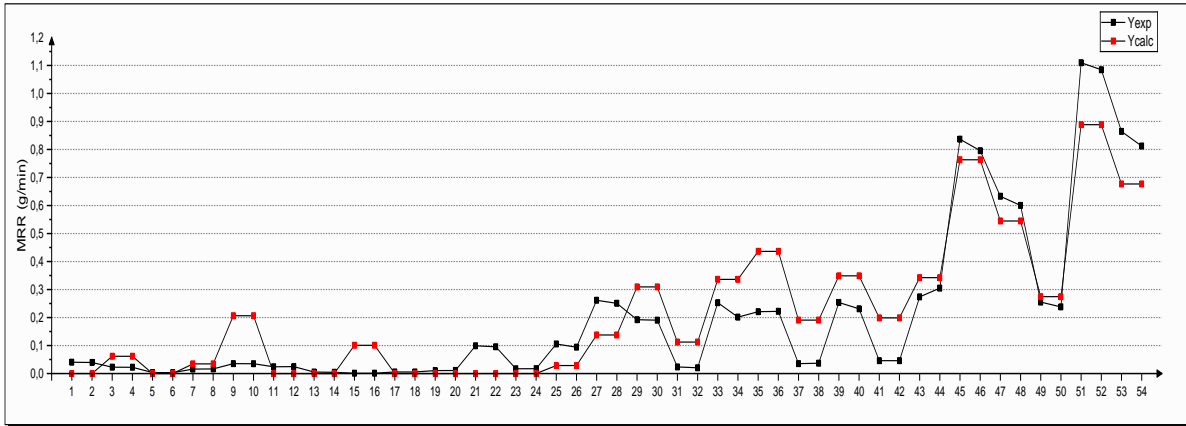


**Figure 14.** Comparison between the measured  $Y_{exp}$  and the predicted  $Y_{calc}$  by the MRR model.

Figures 15, 16 and 17 show the response surfaces associated with the material removed flow model. We have chosen to present the variation of  $(I / Ton)$ ,  $(I / Toff)$  and  $(GAP / AUX)$ , the other factors being fixed at the center of the experimental domain. From the simultaneous two- and three-dimensional representation of the variation in discharge current  $I$  and pulse time  $Ton$  in Figure 15, it can be seen that the minimum of the material flow rate removed is obtained when the values  $I = 4$  A and  $Ton = 4 \mu s$  and the maximum flow is obtained for the values  $I = 10$  A and  $Ton = 12 \mu s$ . The value of MRR increases proportionally with the discharge current  $I$  and the pulse time  $Ton$ .

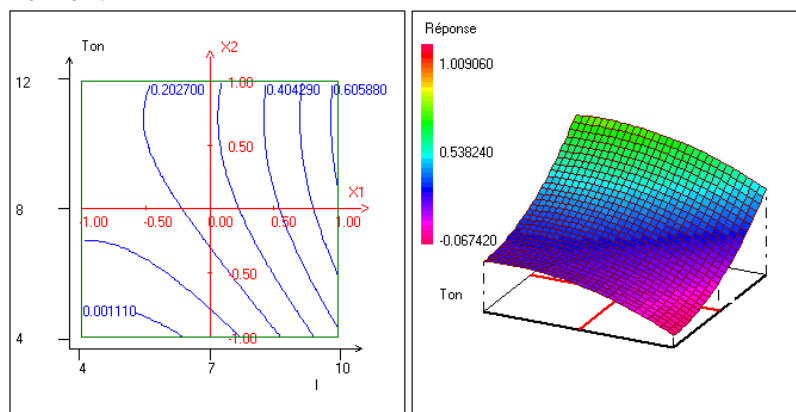


**Figure 15.** 2D and 3D response surface of MRR in the  $I, Ton$  plane.

Variation of MRR response in the  $I, Ton$  plane. Fixed Factors:  $Toff = 6 \mu s$ ,  $GAP = 10 \mu m$ ,  $AUX = 8$ .

From the 2D diagram and the response surface graph in Figure 16 of the variation in discharge current  $I$  and rest time  $Toff$ , we can see:

- the maximum material removal rate for the values of  $Toff = 6 \mu s$  and  $I = 10$  A;
- the minimum material flow for two removes the  $Toff$  values, i.e.  $3 \mu s$  or  $9 \mu s$  and  $I = 3$  A.

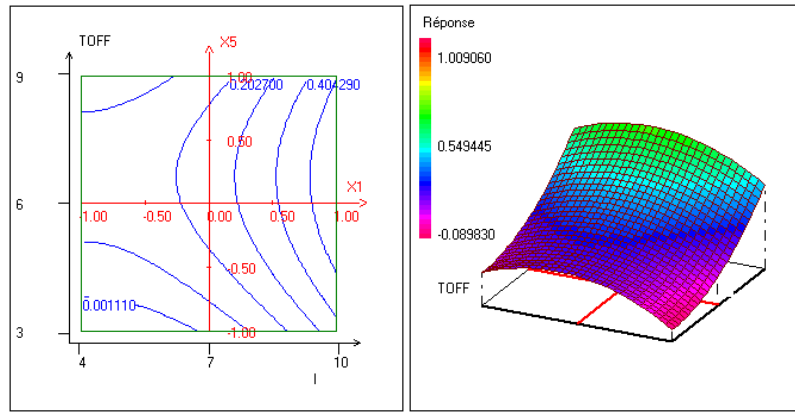


**Figure 16.** 2D and 3D response surface of MRR in the I, Toff plane. Variation of MRR response in plane I, Toff. Fixed Factors: Ton = 8µs, GAP = 10µm, AUX = 8.

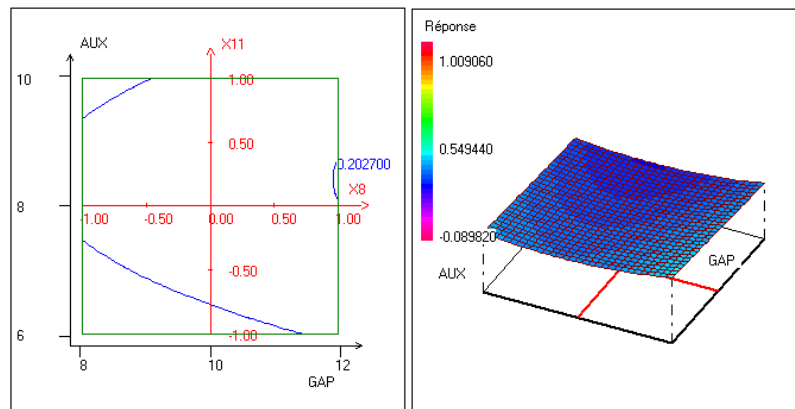


**Figure 17.** 2D and 3D response surface of MRR in the GAP, AUX plane. Variation of the MRR response in the GAP, AUX plan. For the fixed factors: I = 7A, Ton = 8µs, Toff = 6µs.

A small variation is observed when varying the distance between the electrode-work piece (GAP) and the auxiliary protection (AUX) in Figure 17.

### 5.2.3. Modeling of TWR according to parameters and interactions

A third polynomial model is defined of the TWR electrode wear rate as a function of the first and second order parameters with the fixed interactions as shown in Eq. (16).

$$TWR = b_0 + b_1 \times I + b_2 \times Ton + b_3 \times I \times Ton + b_4 \times Toff + b_5 \times I \times Toff + b_6 \times GAP + b_7 \times I \times GAP + b_8 \times AUX + b_9 \times I \times AUX + b_{11} \times I^2 + b_{22} \times Ton^2 + b_{44} \times Toff^2 + b_{66} \times GAP^2 + b_{88} \times AUX^2 \quad (16)$$

The statistical analysis leads us to the study table of the variance of Table 23. It mainly indicates that the determined model is very well fitted, since the sum of the squares of residuals is very small compared to the sum of the regression squares.

**Table 23.** Analysis of variance of TWR.

Source of variation	Sum of squares (SS)	Degrees of freedom (DOF)	Medium square (MS)	Rapport (F)	Signif
<b>Regression (R)</b>	2.45591E+0004	18	1.36440E+0003	<b>55.0365</b>	< 0.01 ***
<b>Residues (E)</b>	8.67677E+0002	35	2.47908E+0001		
<b>Total (T)</b>	2.54268E+0004	53			

From the Fisher table, we deduce:

$$F_{0.05} (DOF_R; DOF_E) = 1.91 < 55.0365$$

$$F_{0.01} (DOF_R; DOF_E) = 2.5 < 55.0365$$

$$F_{0.001} (DOF_R; DOF_E) = 3.38 < 55.0365 (***)$$



The Fisher test makes it possible to demonstrate the existence of a statistically significant difference with a confidence level of 99.9% in Table 22 by the appearance of three stars in front of the significance of the regression, in other words, more the result of the hypothesis test is significant the more robust the model is.

A more detailed analysis of the estimates and statistics of the multiple linear correlation coefficient R2 in Table 24 clearly shows the very good quality of the fit since R2 = 0.966 which is very close to 1.

**Table 24.** Statistics of TWR coefficients.

Standard deviation of the response	4.9790333
R2	0.966
R2A	0.948
R2 pred	0.919
PRESS	2061.393
Number of degrees of freedom	35

Table 25 represents the estimation of the various parameters of the model, for each coefficient of (bi) or (bij), it is possible to test the hypothesis of its nullity. It is interesting to note that all of the interaction effects between the factors appear to be significant.

**Table 25.** Estimation of the model parameters.

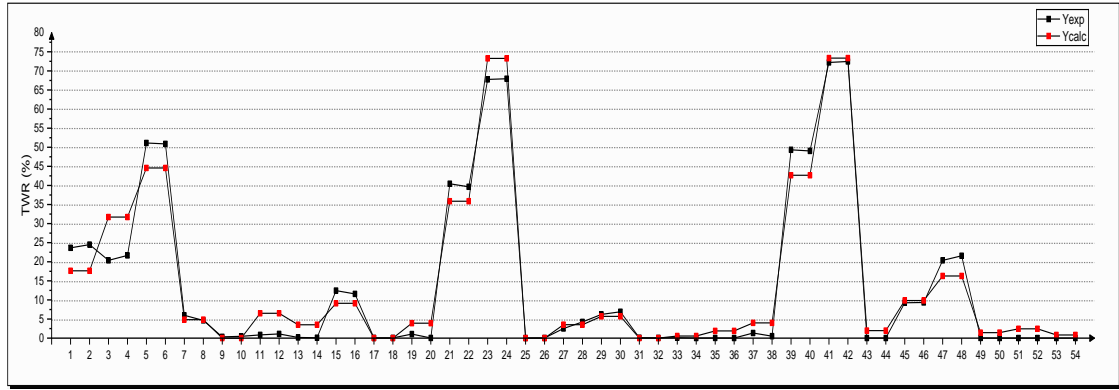
Name	bi	Standard Devi.	ti	Signif. %
b0	4.4965876	2.2472143	2.00	5.3
b1	2.1018455	0.8298389	2.53	1.60 *
b2	-17.4750068	0.8298389	-21.06	< 0.01 ***
b3	2.4896034	0.8298389	3.00	0.495 **
b4	10.4824214	0.8298389	12.63	< 0.01 ***
b5	-3.6640050	0.8298389	-4.42	< 0.01 ***
b6	7.6875799	0.8298389	9.26	< 0.01 ***
b7	-2.8267610	0.8298389	-3.41	0.167 **
b8	9.4413138	0.8298389	11.38	< 0.01 ***
b9	-2.0803749	0.8298389	-2.51	1.70 *
b11	1.7005328	1.4373231	1.18	24.5
b22	13.6435274	1.4373231	9.49	< 0.01 ***
b44	-1.1040170	1.4373231	-0.77	44.8
b66	2.1790636	1.4373231	1.52	13.8
b88	-1.6979927	1.4373231	-1.18	24.5

After checking the hypothesis of their nullities (Eq. 11), the results obtained in Table 25 allow us to write the predicted TWR response as follows:

$$\text{TWR} = 4.4965876 + 2.1018455 \times I - 17.4750068 \times \text{Ton} + 2.4896034 \times I \times \text{Ton} + 10.4824214 \times \text{Toff} - 3.6640050 \times I \times \text{Toff} + 7.6875799 \times \text{GAP} - 2.8267610 \times I \times \text{GAP} + 9.4413138 \times \text{AUX} - 2.0803749 \times I \times \text{AUX} + 13.6435274 \times \text{Ton}^2 \quad (17)$$

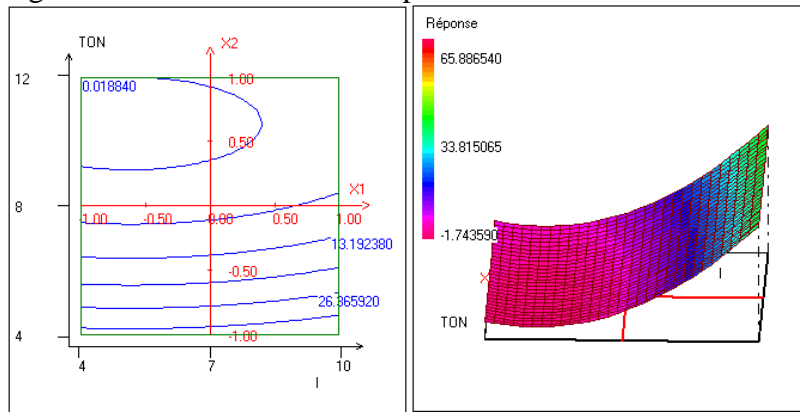
This expression has been simplified by eliminating the effects of interactions and parameters deemed insignificant, to more easily handle the reduced model expression while maintaining goodness of fit.

Figure 18 allows a more precise judgment of the quality of the adjustment made experiment by experiment. The comparison between the  $Y_{\text{exp}}$  (measured responses) and  $Y_{\text{calc}}$  (model predicted responses) curves of (MRR) confirms that the model fits well. It can be noted that the maximum difference between the calculated and experimental values of the electrode wear rate does not exceed 10%.



**Figure 18.** Comparison between the measured  $Y_{exp}$  and the predicted  $Y_{calc}$  by the TWR model.

Figures 19, 20 and 21 show the response surfaces associated with the TWR tool wear rate model. We have chosen to present the variation of (I / Ton), (I / GAP) and (Ton / Toff), the other factors being fixed at the center of the experimental domain.



**Figure 19.** 2D and 3D response surface of MRR in the I, Ton plane.

Variation of the TWR response in the I, Ton plane. Fixed Factors: Toff = 6 $\mu$ s, GAP = 10 $\mu$ m, AUX = 8.

From the representation of the graphs of the variation of discharge current I and pulse time Ton in Figure 19, it can be seen that there is a stationary point approximately at the values Ton = 12  $\mu$ s and I = 4 A with a minimum tool wear rate.

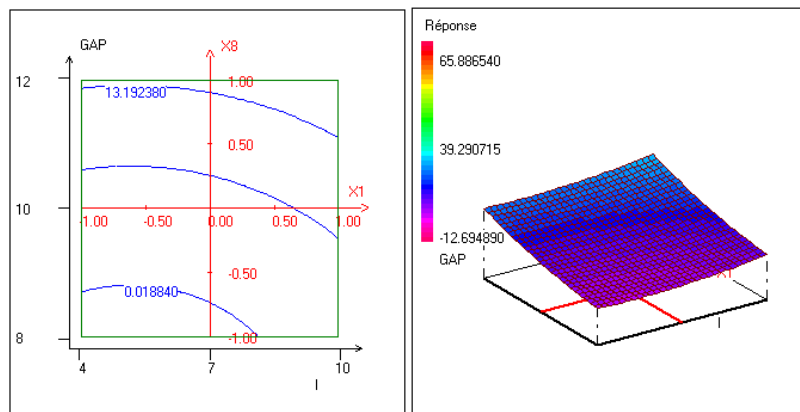


**Figure 20.** 2D and 3D response surface of MRR in the I, GAP plane.

Variation of TWR response in plan I, GAP. Fixed Factors: Ton = 8 $\mu$ s, Toff = 6 $\mu$ s, AUX = 8.

A small variation is observed when varying the two parameters, the discharge current I and the distance between the electrode and the GAP part in Figure 20.

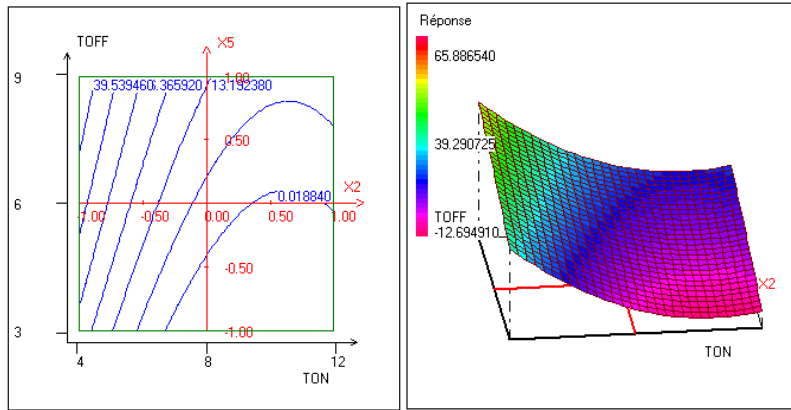


**Figure 21.** 2D and 3D response surface of MRR in the Ton, Toff plane.

Variation of the TWR response in the plane Ton, Toff. Fixed Factors: I = 7A, GAP = 10µm, AUX = 8.

By examining the variation in pulse time Ton and rest time Toff in Figure 21, we can easily see the optimum (minimum) of the electrode wear rate for the values Ton = 12 µs Toff = 3µs.

### 6. MODEL VALIDATION

To validate the models, we performed additional tests in the experimental field at points not tested by the design of experiments, with unused factor levels.

Table 26 shows on the one hand the plan of the validation tests and the results obtained and on the other hand the comparison of the results between the model of Ra and the experimental tests.

**Table 26.** Plan of the validation tests of the Roughness model Ra

N°	Parameters					Ra (µm)				
	I	Ton	Toff	GAP	AUX	Model	Exp.	Difference	Relative error	
1	10	5	9	12	10	3.2	3.460	0.260	0.075	7.5%
2	10	4	5	10	10	2.4	2.668	0.268	0.100	10.0%

Table 27 presents the plan of the validation tests, the results of the experimental tests obtained and the comparison between the MRR prediction model and the experimental tests carried out.

**Table 27.** Plan of validation tests for the model of the material flow removed MRR

N°	Parameters					MRR (g/min)				
	I	Ton	Toff	GAP	AUX	Model	Exp.	Difference	Relative error	
1	10	5	9	12	10	0.1	0.09094	0.00905	0.0995	9.95%
2	10	12	7	10	10	0.9	0.89603	0.00442	0.0442	4.42%

Table 28 presents the plan of the validation tests with the results of the comparison between the prediction model of TWR and that of the experimental tests.

**Table 28.** TWR tool wear rate model validation test plan

N°	Parameters					TWR (%)				
	I	Ton	Toff	GAP	AUX	Model	Exp.	Difference	Relative error	
1	10	5	9	12	10	60	55.142	04.858	0.0880	8.8 %
2	10	4	5	10	10	40	39.767	00.233	0.0058	0.58%

The results of the validation tests of the different models show us that:

- The maximum relative error calculated for the roughness Ra is acceptable since it does not exceed 10%.
- The maximum relative error estimated for the flow rate material removed MRR is equal to 9.95%, but it is acceptable.

- The maximum relative error of the TWR electrode wear rate results is 8.8% so the result is acceptable.

## 7. CONCLUSION

In this study, the influence of die-sinking EDM machining parameters and the influence of interactions between process parameters was investigated using the design of experiments method. The experimental results were used to develop material removal rate (MRR), tool wear rate (TWR) and roughness (Ra) models which were successfully analyzed using the statistical method. (ANOVA).

From the results, it was found that the pulse time (Ton) the idle time (Toff) the discharge current (I) and the sensitivity of the protection against short circuits in the GAP (AUX) play an important role in spark erosion operations. It has been noticed that the interactions of the various parameters Ton, Toff, GAP and AUX with the discharge current are the most significant.

In addition, it was found that the two factors the discharge current I and the pulse time Ton are the most significant factors on the roughness Ra and the MRR. In addition, it has been noticed that the Toff resting time factor is very significant on the tool wear rate.

The main conclusions drawn from the research are as follows:

- the optimal (minimum) level of the factors for the response Ra is obtained for the values of  $I = 4$  A and  $T_{on} = 4$   $\mu$ s. The value of the roughness Ra increases proportionally with the increase in the discharge current I;
- the optimal (maximum) level of the factors for the MRR response is obtained for the values of  $I = 10$  A and  $T_{on} = 12$   $\mu$ s. The value of MRR increases proportionally with the discharge current I and the pulse time Ton;
- the optimal (minimum) level of the factors for the TWR response is obtained for the values of  $T_{on} = 12$   $\mu$ s and  $T_{off} = 3$   $\mu$ s. The value of TWR increases proportionally with increasing discharge current I, increasing rest time Toff and decreasing pulse time Ton.

The polynomial models developed for the three responses are evaluated and validated using the analysis of variance method on the one hand which has been found to be adjusted and on the other hand by the experimental validation tests, the comparison of experimental results with those of theoretical models are conclusive.

## Acknowledgment

The authors gratefully acknowledge the valuable help rendered by ESIM Company for technical support of the experiments and for their constructive comments.

## REFERENCES

- [1]. Meslameni, W., Kamoun, T., Hbaieb, M. (2019). Experimental modeling of EDM process using the experimental design method, *Int J Applied Research and Technology*, 2, 39-47.
- [2]. Agarwal, N., Shrivastava, N., Pradhan, M.K. (2019). Optimization of relative wear ratio during EDM of titanium alloy using advanced techniques, *SN Applied Sciences*, 2, 99. <https://doi.org/10.1007/s42452-019-1877-2>
- [3]. Prathipati, R., Dora, S.P., Chanamala, R. (2020). Wear behavior of wire electric discharge machined surface of 316L stainless steel, *SN Applied Sciences*, 2, 412. <https://doi.org/10.1007/s42452-020-2244-z>
- [4]. Prathipati, R., Ch, R., Dora, S.P. (2019). Corrosion behavior of surface induced by wire EDM on 316L stainless steel: an experimental investigation, *SN Applied Sciences*, 1, 952. <https://doi.org/10.1007/s42452-019-0992-4>
- [5]. Dewan, P.R., Lepcha, L.P., Khaling, A.N., Prasad, N., Rai, S. (2018). Experimental Analysis and Optimization of EDM Process Parameters, *IOP Conf. Series: Materials Science and Engineering*, 377, 012220. doi:10.1088/1757-899X/377/1/012220
- [6]. Kolse, D.M., Shrivastava, R.K. (2017). Effect of Electrode Materials and Optimization of Electric Discharge Machining of M2 Tool Steel Using Grey-Taguchi Analysis, *International Journal of Scientific Research in Science and Technology*, 3(8), 1020-1027.

- [7]. El-Bahloul, S.A. (2020). Optimization of wire electrical discharge machining using statistical methods coupled with artificial intelligence techniques and soft computing, *SN Applied Sciences*, 2, 49. <https://doi.org/10.1007/s42452-019-1849-6>
- [8]. Mohanty, U.K., Rana, J., Sharma, A. (2017). Multi-objective optimization of electro-discharge machining EDM parameter for sustainable machining, *Materials Today: Proceedings*, 4(8), 9147–9157. <https://doi.org/10.1016/j.matpr.2017.07.271>
- [9]. Chandramouli, S., Eswaraiah, K. (2018). Experimental investigation of EDM Process parameters in Machining of 17-4 PH Steel using Taguchi Method, *Materials Today: Proceedings*, 5(2), 5058–5067. <https://doi.org/10.1016/j.matpr.2017.12.084>
- [10]. Satpathy, A., Tripathy, S., Senapati, N.P., Brahma, M.K. (2017). Optimization of EDM process parameters for AlSiC- 20% SiC reinforced metal matrix composite with multi response using TOPSIS, *Materials Today: Proceedings*, 4(2), 3043–3052. <https://doi.org/10.1016/j.matpr.2017.02.187>
- [11]. Parsana, S., Radadia, N., Sheth, M., Sheth, N., Savsani, V., Prasad, N.E., Ramprabhu, T. (2018). Machining parameter optimization for EDM machining of Mg–RE–Zn–Zr alloy using multi-objective Passing Vehicle Search algorithm, *Archives of Civil and Mechanical Engineering*, 8(3), 799-817. <https://doi.org/10.1016/j.acme.2017.12.007>
- [12]. Saffaran, A., Moghaddam, M.A., Kolahan, F. (2020). Optimization of backpropagation neural network-based models in EDM process using particle swarm optimization and simulated annealing algorithms. *Journal of the Brazilian Society of Mechanical Sciences and Engineering*, 42, 73. <https://doi.org/10.1007/s40430-019-2149-1>
- [13]. Subrahmanyam, M., Nancharaiah, T. (2020). Optimization of process parameters in wire-cut EDM of Inconel 625 using Taguchi's approach. *Materials Today: Proceedings*, 23(3), 642-646. <https://doi.org/10.1016/j.matpr.2019.05.449>
- [14]. Mohamed, M.F., Lenin, K. (2020). Optimization of Wire EDM process parameters using Taguchi technique. *Materials Today: Proceedings*, 21(1), 527-530. <https://doi.org/10.1016/j.matpr.2019.06.662>
- [15]. Tlili, A., Ghanem, F. (2018). A numerical investigation on the local mechanical behavior of a 316-L part during and after an EDM basic electrical discharge. *Int J Adv Manuf Technol*. <https://doi.org/10.1007/s00170-018-2618-1>
- [16]. Singh, N.K., Agrawal, S., Johari, D., Singh, Y. (2019). Predictive analysis of surface roughness in argon-assisted EDM using semiempirical and ANN techniques. *SN Applied Sciences*, 1, 995. <https://doi.org/10.1007/s42452-019-1032-0>
- [17]. Abu Qudeiri, J.E., Saleh, A., Ziout, A., Mourad, A.I., Elkaseer, A. (2019). Advanced Electric Discharge Machining of Stainless Steels: Assessment of the State of the Art Gaps and Future Prospect. *Materials*, 12, 907. doi:10.3390/ma12060907
- [18]. Sharma, S., Vates, U.K., Bansal, A. (2021). Parametric optimization in wire EDM of D2 tool steel using Taguchi method. *Materials Today: Proceedings*, 45(2), 757-763. <https://doi.org/10.1016/j.matpr.2020.02.802>
- [19]. Satishkumar, P., Murthi, C.S., Meenakshi, R. (2021). Optimization of machining parameters in wire EDM of OFHC copper using Taguchi analysis. *Materials Today: Proceedings*, 37(2), 922-928. <https://doi.org/10.1016/j.matpr.2020.06.120>
- [20]. Girisha, L., Sridhar, S., Tadepalli, L.D., Swetha, M., Subbiah, R., Marichamy, S. (2021). Performance analysis and taguchi approach on wire cut EDM using microwave sintered chromium composite. *Materials Today: Proceedings*, 45(2), 2105-2108. <https://doi.org/10.1016/j.matpr.2020.09.700>
- [21]. Ganapati, S.T., Pachapuri, M.S.A., Adake, C.V. (2019). Influence of process parameters of electrical discharge machining on MRR, TWR and surface roughness: A review. *AIP Conference Proceedings*, 2148, 030045. <https://doi.org/10.1063/1.5123967>
- [22]. Meslameni, W., Ben Salem, C. (2021). Modeling of the springback in folding using the experimental design method. *Journal of applied research on industrial engineering*, 8(3), 290-308. Doi: 10.22105/JARIE.2021.280059.1284